# 論文 / 著書情報
# Article / Book Information

| | |
|---|---|
| 題目(和文) | |
| Title(English) | Origin of basal stem cells of the epidermis and their regulation during growth, homeostasis, and injury response in zebrafish |
| 著者(和文) | LIUZhengcheng |
| Author(English) | Zhengcheng Liu |
| 出典(和文) | 学位:博士(理学),<br>学位授与機関:東京工業大学,<br>報告番号:甲第12660号,<br>授与年月日:2024年3月26日,<br>学位の種別:課程博士,<br>審査員:川上 厚志,田中 幹子,粂 昭苑,立花 和則,山口 雄輝 |
| Citation(English) | Degree:Doctor (Science),<br>Conferring organization: Tokyo Institute of Technology,<br>Report number:甲第12660号,<br>Conferred date:2024/3/26,<br>Degree Type:Course doctor,<br>Examiner:,,,, |
| 学位種別(和文) | 博士論文 |
| Type(English) | Doctoral Thesis |

**2023 Doctoral dissertation**

# Origin of basal stem cells of the epidermis and their regulation during growth, homeostasis, and injury response in zebrafish

**Tokyo Institute of Technology**
**Graduate School of Life Science and Technology**
**Department of Life Science and Technology**
**Kawakami Laboratory**

**Zhengcheng Liu**

**Advisor: Atsushi Kawakami, Associate Professor**

# Contents

# Abstract

**Introduction**

The basal stem cells of the epidermis are essential to maintain epidermal homeostasis and regenerate the lost tissue when the skin is injured. Whereas mammals have the limited capability to repair the skin with scar formation, some vertebrate species such as teleost fish can perfectly regenerate the skin without any scar even after fin amputation (Yoshinari and Kawakami, 2011). In the previous study of zebrafish fin regeneration, it was suggested that the epidermis is regenerated by the self-renewal of the basal cells (Shibata et al., 2018); however, the cells in the wound epidermis (WE) mostly disappeared after regeneration. Unfortunately, the previously established transgenic line *Tg(fn1b:creERt2)* only labels the WE cells, we were not able to track the fate of the basal cells in the skin homeostasis. Thus, the origin and lineage fate of the basal cells are still largely unknown. This study aimed to establish new *Tgs* to globally label the basal cells and reveal their developmental origin and fates throughout life.

**Methods and Results**

From the previous RNA sequencing data and related research (Yoshinari et al., 2009; DeWard et al., 2014; Wehner et al., 2014), I selected *itgb4* and *krt18* as the markers of the basal cells in the epidermis. The *in situ* hybridization (ISH) analysis confirmed that the *itgb4* is always expressed in the basal cells of the epidermis, while the *krt18* is only detected in the basal cells of the regenerating epidermis. I established the *Tg(itgb4:creERt2)* and *Tg(krt18:creERt2)* to label the basal cells in the homeostatic and regenerative epidermis.

To investigate the origin of the adult basal cells during developmental stages, I first examined the expressions of *krt18*, *itgb4,* and *krt4*, which is a marker of keratinocytes by ISH. The results showed that *krt4* and *krt18* are uniformly expressed in the epidermis before the somite stage. But, their expressions became mosaic in the somite stage. The expression of *itgb4* was only detected from 1 dpf, whereas the *krt18* expression declined at 1 dpf and thereafter.

To determine the timing of basal cell fate specification, I labeled the *krt18*$^{+}$ and *krt4*$^{+}$ cells at the pre-somite stage and somite stage and tracked their fate until the 3-month-old adult stage. I found both *krt18*$^{+}$ and *krt4*$^{+}$ cells at the pre-somite stage contributed to the adult epidermis but those cells labeled at the somite stage mostly disappeared during larval and juvenile growth stages. On the other hand, the *itgb4*$^{+}$ cells labeled at 1 dpf contributed to the adult epidermis, indicating that the fate segregation of adult basal cells occurs at the somite stage, and a fraction of the epithelial cells with decreased *keratin* gene expressions become the *itgb4*$^{+}$ basal progenitor cells. I further showed by RNA profiling that they already have a basal cell identity.

Next, to examine the behavior of basal cells during the juvenile growth stage, I labeled the *itgb4*$^{+}$ basal cells and tracked their fates. I showed that the labeled basal cells actively become transit amplifying cells (TACs) to generate many keratinocytes or undergo self-renewal to slowly expand the basal cells. However, most of the basal cells became quiescent in the adult stage. These observations are consistent with those of the mammalian epidermis and suggested that the zebrafish is a good model to reveal the regulative mechanism of skin homeostasis.

I further examined whether self-renewal and differentiation can be induced by skin injuries. To do this, I established additional *Tgs* in which the TagBFP-nfsB fusion protein is expressed under the *itgb4* or *krt4* promoter. The basal cells or non-basal keratinocytes are specifically injured in these *Tgs* by the treatment with Mtz (metronidazole). Combining with the Cre-mediated basal cell labeling, I found the labeled basal cells were induced to differentiate into the TACs/keratinocytes, but rarely self-renewed, by the non-basal keratinocyte ablation. Conversely, the basal cells underwent self-renewal by basal cell ablation. I further found that the *krt18* expression in the basal cells was induced by the injury to the basal cells, suggesting that the basal cell self-renew occurs by way of the *krt18*$^{+}$ state.

**Discussion**

My study provided a comprehensive understanding of the origin and behavior of the basal cells in growth, homeostasis, and injury response. The established *Tgs* and my data will be a useful basis to study the regulation of epidermal basal cells in homeostasis and regenerative situations. In the future study, it will be interesting to reveal the mechanism and signals for basal cell fate decisions within the embryonic epithelial cells and the wound-sensing and controlling mechanism by which the basal cells take either differentiation or self-renewal.

**References**

**Yoshinari, N. and Kawakami, A.** (2011). Mature and juvenile tissue models of regeneration in small fish species. *The Biological Bulletin* **221**, 62-78.

**Shibata, E., Ando, K., Murase, E. and Kawakami, A.** (2018). Heterogeneous fates and dynamic rearrangement of regenerative epidermis-derived cells during zebrafish fin regeneration. *Development* **145**, dev162016.

**Yoshinari, N., Ishida, T., Kudo, A. and Kawakami, A.** (2009). Gene expression and functional analysis of zebrafish larval fin fold regeneration. *Developmental Biology* **325**, 71-81.

**DeWard, A. D., Cramer, J. and Lagasse, E.** (2014). Cellular heterogeneity in the mouse esophagus implicates the presence of a nonquiescent epithelial stem cell population. *Cell Reports* **9**, 701-711.

**Wehner, D., Cizelsky, W., Vasudevaro, M. D., Özhan, G., Haase, C., Kagermeier-Schenk, B., Röder, A., Dorsky, R. I., Moro, E. and Argenton, F.** (2014). Wnt/β-catenin signaling defines organizing centers that orchestrate growth and differentiation of the regenerating zebrafish caudal fin. *Cell Reports* **6**, 467-481.

**Conference presentations**

○Zhengcheng Liu, Yidan Meng, and Atsushi Kawakami. “Study of epidermal homeostasis and regeneration by long-term lineage tracing of basal stem cells in zebrafish” The 74th Zoological Society of Japan (2022, 3/5, Zoom, Online)

○Zhengcheng Liu, Yidan Meng, and Atsushi Kawakami. “Origin and lineage of the basal stem cells of the epidermis in zebrafish fin.” The 55th Annual Meeting of the Japanese Society for Developmental Biology (2022, 5/31-6/3, Kanazawa)

○Zhengcheng Liu, Yidan Meng, Atsushi Kawakami. “Origin and lineage of the basal stem cells of the epidermis in zebrafish” The 28th Japanese Medaka and Zebrafish Meeting (2022, 9/1-9/2, Oosaka)

○Zhengcheng Liu, Yidan Meng, Ayu Ishikura, and Atsushi Kawakami. “Origin of epidermal basal stem cells and their behavior during homeostasis and injury responses in zebrafish” The 56th Annual Meeting of the Japanese Society for Developmental Biology (2023, 7/22-7/25, Sendai)

# Abbreviations

AO: acridine orange

aPKC: atypical protein kinase C

BCIP: 5-bromo-4-chloro-3-indolyl-phosphate

BFP: blue fluorescent protein

BMP: bone morphogenetic proteins

BSA: bovine serum albumin

CreERt2: Cre recombinase with a mutated tamoxifen-responsive estrogen

*cryaa*: crystalline alpha A

DABCO: 1,4-diazabicyclo-[2,2,2,] octane

DAPI: 4',6-diamidino-2-phenylindole

DEG: differentially expressed gene

DIG: digoxigenin

Dpa: day(s) post amputation

Dpt: day(s) post treatment

Dpl: day(s) post labeling

DsRed2: discosoma red fluorescent protein 2

EdU: 5-ethynyl-2´-deoxyuridine

EGFP: enhanced green fluorescent protein

ER: estrogen receptor

EVL: enveloping layer

FGF: fibroblast growth factor

Hpa: hour(s) post amputation

HB: hybridization buffer

HF: hair follicles

ICI: fulvestrant, ICI-182780

IFE: interfollicular epidermis

ISH: *in situ* hybridization

*itgb4*: integrin β4

*krt4*: keratin 4

*krt18*: keratin 18

*krtt1c19e*: keratin type 1 c19e

MeOH: methanol

Mtz: metronidazole

NBT: nitro blue tetrazolium

Nfatc1: nuclear factor of activated T cells 1

NfsB*:* oxygen-insensitive NAD(P)H nitroreductase

NTR*:* nitroreducatase

*olactb*: oryzias latipes β-actin

PBT: phosphate buffered saline with Tween20

PBTx: phosphate buffered saline with Triton X 100

PFA: paraformaldehyde

ProK: proteinase K

*p63*: transformation-related protein 63

SEM: standard error of the mean

SSC: saline sodium citrate

TAC: transit-amplifying cells

TAM: 4-hydroxy tamoxifen

*Tg*: transgenic

Tricaine: 3-aminobenzoic acid ethyl ester

WE: wound epidermis

Wnt: wingless-related integration site

WT: wild-type

# Chapter 1 Introduction

## 1.1. The structure and function of the epidermis

### 1.1.1. The epidermis of mammals

The epidermis is the outermost tissue of the skin that protects internal tissues and organs throughout life. They have a flexible and multilayered architecture that covers the entire body and prevents water loss and/or damage (Rawlings and Harding, 2004). From the transverse section of the mammalian epidermis, different layers from inner to outer side can be seen: stratum basale, stratum spinosum, stratum granulosum, and stratum corneum (Fig. 1A) (Barbieri et al., 2014). The stratum basale is the most-inner layer of the epidermis, which contains the epidermal stem cells, merkel cells, and melanocytes; the stratum spinosum consists of 8-10 layers of keratinocytes and Langerhans cells; the stratum granulosum is composed of 3-5 layers which are rich in keratohyalin and lamellar granules; and the stratum corneum is the most outer layer that consists flattened, dead keratinocytes (Fig. 1B) (Wickett and Visscher, 2006; Barbieri et al., 2014; Yousef et al., 2022). Among multiple types of epidermal cells, the most abundant keratinocytes are important as a water barrier that secrete lipids and regulate calcium absorption. The basal stem cells are essential to continuously produce these keratinocytes to maintain the epidermis integrity during the whole lifespan (Mascré et al., 2012; Yousef et al., 2022). The other types of epidermal cells such as melanocytes paly roles in UV protection, the Langerhans cells are essential for immune response, and merkel cells serve a sensory function as mechanoreceptors for light touching (Yousef et al., 2022).

### 1.1.2. The epidermis of teleost fish

Some vertebrates like teleost fish, have a conserved and similar architecture and turnover cycles of epidermis compared with mammals (Chen et al., 2016). For example, the adult

zebrafish epidermis is composed of three main layers: the basal, suprabasal, and superficial layers are localized from inner to outer on the basal membrane (Fig. 2) (Henrikson and Gedeon Matoltsy, 1967a, b, c; Chang and Hwang, 2011). Similar to mammals, fish basal cells serve as stem cells for epidermal homeostasis and regeneration (Lee et al., 2014), and cells in the suprabasal layer contain keratinocyte precursors, and various types of cells including mucous cells, club cells, sensory cells, and ionocytes. The mucous cells produce the antifungal and antibacterial mucus; the club cells release alarm signaling factors to response to fright reaction; ionocytes act as ion transporters to maintain the homeostasis of body fluids; and the sensory cells play roles in sensing the stimuli from the external environment (Le Guellec et al., 2003; Chang and Hwang, 2011; O'Brien et al., 2012). However, different from the mammalian skin, the outermost superficial layer in fish skin is composed of living cells, rather than dead cells (Le Guellec et al., 2003).

## 1.2. Epidermis development, homeostasis, and regeneration

### 1.2.1. Development of epidermis

During embryonic development, both mammalian and zebrafish skin is derived from a single cell layer. In mammals, the initial single-layered epithelium is derived from the ectoderm, and stratified to become two layers around embryonic day (E) 9.5 with regulation of *p63* (Smart, 1970; Koster and Roop, 2004). Then the suprabasal layers are generated from the basal cells around E12.5 and further differentiated to generate the fully functional epidermis by E17.5 (Hardman et al., 1998; Blanpain et al., 2006). In the case of zebrafish epidermis, the monolayer named enveloping layer (EVL) is formed following gastrulation and the basal epidermal layer appears later during gastrulation (Kimmel et al., 1990; Bakkers et al., 2002). Therefore, a bi-layered embryonic epithelium is formed as early as 24 hours post-fertilization (hpf). Subsequently, the basal cells produce many differentiated keratinocytes and thicken the epidermis becoming 3 layers by 15 dpf and further becoming 4 layers by 26 dpf (Le Guellec et al., 2003; Lee et al., 2014).

### 1.2.2. Tissue maintenance of the homeostatic epidermis

The epidermal stem cells which are localized in the basal epidermal layer are the key to maintaining the tissue by balancing their self-renewal and differentiation (Mascré et al., 2012). In recent studies, it has been suggested that the basal stem cells undergo both asymmetric and symmetric division in the mammalian homeostatic epidermis (Fig. 3) (Fuchs, 2008; Niezgoda et al., 2017). In the mouse embryonic epidermis, ~70% of basal cells undergo asymmetric division to produce a stem cell and a suprabasal cell, whereas ~30% undergo symmetric division to produce two basal cells (Lechler and Fuchs, 2005). Moreover, lineage fate tracing experiments in adult mouse skin also provided more evidence to support that both asymmetric and symmetric divisions are orchestrated during skin homeostasis (Clayton et al., 2007; Mascré et al., 2012; Koren et al., 2022). Besides, the slow-cycling stem cells and the fast-cycling transit-amplifying cells (TACs) were identified by Cre-mediated cell lineage tracing in mice epidermis (Mascré et al., 2012; Koren et al., 2022). The *thy1*$^{+}$ stem cells occasionally produce the *thy1*$^{-}$ TACs, which have fast cycling to produce differentiated keratinocytes. Thus, the TACs always fated to disappear, whereas the *thy1*$^{+}$ stem cells are the key to maintaining the epidermis during a long lifespan (Fig. 4) (Koren et al., 2022). However, whether the fish skin has a conserved mechanism to keep maintenance like mammals is still an open question.

### 1.2.3. Regeneration of the epidermis

Despite similar architecture and cellular turnover cycles in mammals and zebrafish epidermis, zebrafish have a strong ability to perfectly regenerate their skin even after fin amputation (Chen et al., 2016; Shibata et al., 2018). The fate of wound epidermis (WE) has been revealed by Cre-mediated cell lineage tracing (Shibata et al., 2018). The WE cells contribute to the regenerated epidermis by undergoing both basal cell self-renewal and keratinocyte differentiation and attain complete epidermal regeneration without scar formation (Shibata et al., 2018). Thus, basal cell behavior is likely the key to complete

regeneration in fish. However, mammals like humans have a limited capacity to repair the wound skin under severe injuries, usually remaining fibrous tissue as known as a scar. It has been proposed that the inflammation that occurs at the wound site initially induces the proliferation of fibroblasts and epidermal keratinocytes and that the fibroblasts transit to myofibroblasts and deposit excess extracellular matrix (ECM) including collagens, leading to impaired keratinocyte migration and re-epithelialization (Woodley et al., 1993; Ghahary et al., 1996; Opalenik and Davidson, 2005).

## 1.3. Origin and behavior of the basal stem cells of the epidermis

### 1.3.1. Origin of adult epidermal stem cells

The epidermal stem cells in the basal epidermal layer are required for skin homeostasis and regeneration. The mammalian skin is composed of hair follicles (HF), sebaceous glands, and interfollicular epidermis (IFE). It has been shown that several stem cell populations exist in HF, sebaceous glands, and IFE, respectively (Blanpain and Fuchs, 2009). All of these epidermal stem cells are derived from a single embryonic surface layer as known as neuroectoderm after gastrulation (Fig. 5) (Gaspard and Vanderhaeghen, 2010; Benitah and Frye, 2012). Successively, the epidermal stem cell fate is determined by the expression of BMP and Wnt signaling (Wilson and Hemmati-Brivanlou, 1995; Wilson et al., 2001). As for zebrafish skin, similar to mammals, the basal progenitor cells are generated from the non-neural ectoderm following gastrulation (Bakkers et al., 2002). It has been reported that the polarization of basal and superficial layers is mediated by aPKC and E-cadherin (Arora et al., 2020).

### 1.3.2. Heterogeneity of the basal stem cells

It was initially hypothesized that the entire basal layer of the epidermis only contained stem cells (Potten et al., 1979). However, more and more evidence was shown to support the heterogeneity of the epidermal basal cells by cell-lineage tracing experiments in recent

decades (Ito et al., 2005; Snippert et al., 2010; Page et al., 2013). In the mammalian hair follicle, *k15*, *k19*, *lgr5*, *tcf3*, *gli1, lgr6*, and *lrig1* expressed cells were identified with different lineage fates and localizations in the basal layer (Fig. 6) (Goodell et al., 2015). Not only HF but also IFE and sebaceous gland have been suggested that include populations of stem cells with heterogeneous fates (Horsley et al., 2006; Page et al., 2013). In addition, Shibata et al. (2018) have shown the heterogeneous fates of *fn1b*$^{+}$ WE cells, which include a part of basal stem cells. Moreover, a recent study has revealed genetic heterogeneity in the basal layer of the fin epidermis during regeneration by single-cell sequencing (Hou et al., 2020).

### 1.3.3. Quiescent state of the adult stem cells

Other than the proliferative stem cells, the quiescent state of adult stem cells has been widely observed in various organs or tissues including skin, gut, and bone marrow (Li and Clevers, 2010; Cheung and Rando, 2013). The quiescent state is thought to be essential for maintaining stemness during a long lifespan, and dysregulation of quiescent often causes an imbalanced production of progenitor cell populations and exhaustion of stem cells (Orford and Scadden, 2008). Thus, investigation of the mechanisms of stem cells entering or exiting the quiescent state and their regulations are important for studying tissue regeneration and maintenance.

## 1.4. Zebrafish: a useful model to study the tissue regeneration

### 1.4.1. Structure of the caudal fin and the regeneration

Zebrafish has become a popular model for studying skin regeneration in the last decades because the fish skin has a similar structure to mammalian, and its transparent character helps visualize the epidermal cells in vivo (Chen et al., 2016; Tan et al., 2023). Besides, the zebrafish caudal fin has been widely used as an ideal model for studying epimorphic regeneration (Yoshinari and Kawakami, 2011). The caudal fin is the largest external

appendage which is located at the posterior end of the body. It has a simple architecture but contains many tissues like fin-ray bones, epithelium, vessels, and mesenchymal cells (Fig.7) (Kawakami, 2010). Unlike mammalian skin repairing with scar formation, the caudal fish fin can perfectly regenerate without any scar formation within 2 weeks (Kawakami, 2010). During the process of regeneration in zebrafish fin (Fig. 8), the epithelial cells near the wound site quickly sealed the opening trauma. Then, the wound epidermis (WE), a specialized epidermal tissue that is crucial for regeneration, is formed immediately by epithelial cell migration (Poss et al., 2000; Kawakami et al., 2004). In the successive stages, the proliferative mesenchymal cells called blastema, are formed at the amputation site and provide an adequate number of cells to compensate for the lost tissue part. Lastly, further cell differentiation and tissue remodeling contribute to the final restoration of the fin to its original size (Kawakami, 2010).

### 1.4.2. Cre-*lox*P system for lineage tracing in the zebrafish model

In the past decades, Cre-*lox*P mediated genetic lineage tracing become a popular approach to analyzing cell behavior and fate during regeneration. Such analyses based on the Cre-*lox*P recombination are achieved by the improved technics of cell labeling and living imaging.

The Cre-*lox*P recombination system was initially founded by Sternberg and Hamilton (1981). They successfully isolated the protein from the P1 bacteriophage that recombines DNA fragments and named it Cre. In addition, the Cre-binding sites of the nucleotides are called *lox*P, the *locus of crossing over* P1. This gene-editing tool has become a popular strategy in genetic and cell biology research. For the operation of the Cre-*lox*P system, a transgenic cell line or animal line which is engineered to carry two 34-bp *lox*P DNA motifs are required (Sauer and Henderson, 1988). When the Cre protein is expressed in the cell or tissue, the target floxed locus in the entire cellular lineage will be recombined (Gu et al., 1993).

Further, an inducible method that controls the timing of recombination has been developed by Feil et al. (1997). This method uses the fusion protein of Cre with estrogen receptor ligand biding domain (ER) with amino acid substitutions at two sites (ERt2). The entrance of the ER or ERt2 to the nucleus is prevented due to Hsp90 binding (Hayashi and McMahon, 2002). But, a small molecule, 4-OH-tamoxifen (TAM) works as a 'switch' that disrupts the interaction of Hsp90 with ERt2. Thus, the Cre-ERt2 fusion protein eventually enters the nucleus to induce recombination (Brocard et al., 1997; Indra et al., 1999).

At present, the Cre-*lox*P system is widely used in many conditional and inducible experiments including gene functional researching (Kos, 2004), cell lineage tracing (Fig. 9) (Ando et al., 2017; Shibata et al., 2018), specific cell depletion (Buch et al., 2005) and so on.

### 1.4.3. NTR-Mtz system for specific ablation in the zebrafish model

In addition to the Cre-*lox*P system and cell fate tracking, the ablation of specific cells is a useful approach for analyzing the functions of these cells. Methods like physical surgery and laser-mediated ablation have also been used for removing the cells (Rompolas et al., 2013). However, these approaches are time-consuming, labor-intensive, and most importantly unstable for reproducibly ablating the specific cell groups (Gahtan and Baier, 2004).

The genetic approach is an alternative way for cell ablation based on diphtheria toxin A-chain (DTA) has been developed (Han et al., 2000). However, the DTA usually causes unintended cell death due to its high toxicity.

An effective conditional ablation technique using the nitroreductase (NTR) and prodrug, metronidazole (Mtz), was established by Lindmark and Müller (1976) and optimized by Grohmann et al. (2009). The Mtz is reduced by the NTR and converted into a potent DNA cross-linking agent that causes cell apoptosis (Curado et al., 2007) (Fig. 10). This method has been successfully used in zebrafish (Chen et al., 2011; Ando et al., 2017; Karttunen and Lyons, 2019; Pourghadamyari et al., 2019).

## 1.5. Aim of this study

As zebrafish is an ideal model to study the cell lineage in vivo, it helps to uncover the mechanism of skin maintenance and regeneration. Shibata et al. (2018) established *Tg(fn1b:creERt2)* to track the fate of WE, however, it is only possible to partially label the basal cells during regeneration and most of the *fn1b*-labeled cells have the disappeared fate. So we were not able to perform a comprehensive analysis of fate tracking on the basal cells during natural growth and homeostasis. Thus, my study aimed to establish new *Tgs* that globally label the basal cells and reveal the origin and fate of stem cells of the epidermis during growth, homeostasis, and injury response.

# Chapter 2 Materials and Methods

## 2.1. Fish husbandry and established strains

Fish were maintained in a recirculating water system in a 14 hrs day/10 hrs night photoperiod at 28.5 °C. The wild-type zebrafish (*Danio rerio*) strain used in this study was originally derived from the Tubingen strain and has been maintained in our facility for more than 10 years by inbreeding. The powder food (Gemma Micro ZF 150, Funakoshi) and brine shrimp for feeding were adjusted with the fish growing size. The embryos were incubated in the egg water (0.06% artificial marine salt, 0.0002% methylene blue). At 5 dpf, the larval fish were transferred into the recirculating water system and fed with powder food. The *Tg(krt4:mcherry-t2a-creERt2)* and *Tg(Olactb:loxP-dsRed2-loxP-egfp)* were established in our laboratory (Yoshinari et al., 2012; Shibata et al., 2018).

All surgeries were performed under 0.002% tricaine (3-aminobenzoic acid ethyl ester, Sigma-Aldrich) anesthesia, and every effort was made to minimize suffering. All animal experiments were performed in strict accordance with the recommendations of the Act on Welfare Management of Animals in Japan and the Guide for the Care and Use of Laboratory Animals from the National Institute of Health. All the animals were handled in accordance with the Animal Research Guidelines of the Tokyo Institute of Technology. The study protocol was approved by the Committee on Ethics of Animal Experiments at the Tokyo Institute of Technology.

## 2.2. Plasmid constructs

The respective Cre constructs, *pTol2(cryaa:egfp;itgb4:mcherry-t2a-creERt2)* and *pTol2(cryaa:egfp;krt18:mcherry-t2a-creERt2)* were made by replacing with the *krt4* promoter of *pTol2(krt4:mcherry-t2a-creERt2)* (Shibata et al., 2018) with −4.5kb *itgb4* or −3.8kb *krt18* promoters at *SfiI* and *FseI* sites. The *crystallin alpha A (cryaa):egfp* cassette was inserted into the EcoNI site, upstream of the promoter. *pTol2(itgb4:mcherry)* and

*pTol2(krt18:mchery)* were prepared by replacing the *sp7* promoter of *pTol2(sp7:mcherry)* (Ando et al., 2017) with the -4.5k *itgb4* and -3.8k *krt18* promoter sequences, respectively, at *SfiI* and *AgeI* sites. The *pTol2(itgb4:tagBFP-nfsB)* and *pTol2(krt4:tagBFP-nfsB)* were made by replacing the *mcherry-t2a-creERt2* sequence of *pTol2(hsp70l:mcherry-t2a-creERt2)* (Yoshinari et al., 2012) with *tagBFP-nfsB*, and then further replaced the promoter sequence with -4.5kb *itgb4* and -4.3kb *krt4* promoter sequences, respectively, at *SfiI* and *AgeI* sites. The underlined portions of the primers denote the restriction enzyme recognition sites for cloning.

| **Primers for amplification of promoters** | | | |
|---|---|---|---|
| *krt4*-pro (-4.3k) | F | *SfiI* | 5'-ggccagatgggccTGCTGATTCTGGCCCGGTAGCT-3' |
| | R | *AgeI* | 5'-accggtGATGCCTGTGTCTTTGAGTTGCTGA-3' |
| *krt18-pro* (-3.8 k) | F | *SfiI* | 5'-ggccagatgggccCAGGACATCTGCCCTCCAGCAC-3' |
| | R | *FseI* | 5'-ggccggccGGTGTAAGTGAGCAGACGAGTG-3' |
| | R | *AgeI* | 5'-accggtGGTGTAAGTGAGCAGACGAGTG-3' |
| *itgb4*-pro (-4.5k) | F | *SfiI* | 5'-ggccagatgggccGTGTTTGTGTGTGTACCTGTGCATGCATGTGCAG-3' |
| | R | *FseI* | 5'-ggccggccCAGTCTGAAACACAAGAGCGAGATCAC-3' |
| | R | *AgeI* | 5'-accggtCAGTCTGAAACACAAGAGCGAGATCAC-3' |

## 2.3. Embryo injection

For preparing the zebrafish embryos, the eggs were collected as early as possible and dechorionated with the 2 mg/ml Pronase (Roche) treatment for several minutes. After washing with egg water several times, the dechorionated embryos were incubated in the 0.3x Niu-Twitty buffer (17.4 mM NaCl, 0.21 mM KCl, 0.12 mM $MgSO_4$, 0.18 mM $Ca(NO_3)_2$, 1.5 mM HEPES, pH 7.6) ready for injection.

The plasmid DNA was purified by QIAprep Spin Miniprep Kit (Qiagen). The purified constructs were injected into one-cell-stage zebrafish embryos with 25 ng/μL transposase mRNA, 0.2M KCl, and 0.25% phenol red at a concentration of 25–40 ng/μL.

The F0 founders were either incrossed or outcrossed to screen for their F1 careers. The following primers were used to amplify the promoter sequences from the genome.

## 2.4. Whole mount *in situ* hybridization (ISH)

Whole-mount ISH was performed according to the standard protocols (Thisse and Thisse, 2008). The DNA templates for the respective probes were amplified from cDNA using KOD Plus Neo (Toyobo) and the primers listed below. The underlined portions of the primers denote the T7 promoter. RNA probes were synthesized using a DIG RNA Labeling Kit (Sigma-Aldrich).

| **Primers for the synthesis of RNA probes** | | |
|---|---|---|
| *itgb4* | F | 5'-ATGGGAGGATGGGCGATACGTCTGGCTGTGGGGAT-3' |
| | R | 5'-taatacgactcactatagggGTCAGCCTGGTTGACCTTACACACGGGCTCTTCTC-3' |
| *krt18* | F | 5'-ATGTCCTGTGCTCTGCTCTGCTGTGTTACTGAGC-3' |
| | R | 5-taatacgactcactatagggTTCAGCTCCAGCTTGCTGTTGGCCTGCTCCAGGA-3' |
| *krt4* | F | 5'-ATGTCAACCAGGTCTATCACCTACTCCAGCGGTGG-3' |
| | R | 5'-taatacgactcactatagggATAGCGTTTACTGCTGACGGTGGTGACACTGG-3' |

Collected samples were fixed by 4% paraformaldehyde (PFA, Sigma Aldrich) / Phosphate Buffered Saline (PBS, 137 mM NaCl, 2,7 mM KCl, 10 mM $Na_2HPO_4$, 1.76 mM $KH_2PO_4$) overnight at 4°C. Then, the samples were washed with 0.1% Tween 20/ PBS (PBT) for 5min (3 times), and gradually dehydrated by 25%, 50%, 75%, and 100% MeOH/PBT for 5 min in each step. When the solution was completely changed to 100% MeOH, the samples were stored at -30°C overnight. Then the samples were kept at room temperature and rehydrated by changing solution with 25%, 50%, 75%, and 100% PBT/MeOH for 5 min in each step. After rehydration, the samples were treated with 10 μg/ml ProK/PBT for 20 min, and washed with PBT for 5 min (2 times). And the samples were immersed in the Hybridization Buffer (HB, 50% formamide, 5x SSC (pH 7.0), 500 ug/ml torula (yeast) RNA or tRNA 50 ug/ml heparin, 0.1% Tween 20, 9mM citric acid to

pH 6.0-6.5) at 65-70ºC for more than 2 hours. And the solution was changed with the HB including 1 μg/ml RNA probes and kept at 70ºC overnight. Then the samples were washed with 25%, 50%, 75%, and 100% 2x SSC/HB solution for 5 min in each step at 65-70 ºC. The 20x Saline Sodium Citrate (20x SSC, Nacalai Tesque) is composed of 3M NaCl, 0.3 M Sodium Citrate, pH 7.0. Next, the 2x SSC and 0.2x SSC were used for washing samples at 65-70 ºC for 10 min, and wait the samples to return to room temperature. Then the samples were washed with 25%, 50%, 75%, and 100% PBT/ 0.2xSSC for 5 min in each step, and the solution was changed to Blocking buffer (2 mg/ml BSA, 5% sheep serum /PBT) for 2 hours at room temperature. Next, the alkaline phosphatase-conjugated anti-DIG antibody was diluted 4000 times in the blocking buffer and kept the samples at 4ºC overnight for reaction. After several times washing by PBT, NTMT buffer (50mM $MgCl_2$, 0.1M Tris-HCl, 0.1M NaCl, 0.1% Tween 20) was treated to the samples for 5 min (3 times). Then the solution was changed with fresh NTMT buffer including 450 μg/ml nitro blue tetrazolium (NBT) and 175 μg/ml 5-bromo-4-chloro-3-indolyl-phosphate (BCIP). After 30 min-6 hours reaction in the dark at room temperature, until the signals become visible, the samples were washed with PBT several times for 5 min and fixed in 4% PFA/PBS. For imaging, the samples were mounted in 80% glycerol and observed under microscopy.

## 2.5. Cre-mediated cell labeling

*Tg* strains carrying the *itgb4:creERt2* or *krt18:creERt2* were crossed with the RSG reporter *Tg* (Yoshinari et al., 2012) to generate double *Tg* lines. Cre-*lox*P recombination was induced by treating double *Tgs* with 4-OH tamoxifen (TAM, Sigma-Aldrich) or Fulvestrant (ICI, Sigma-Aldrich). The recombination conditions are shown in the figure legends. Generally, for single-cell tracking, recombination is induced with 0.5 μM ICI a 30 min. For maximum labeling, recombination was induced with 1 μM TAM for 24 hrs. The treated fish were kept in fresh water in an aquarium for at least four days and used for cell tracing.

## 2.6. Cell tracking and quantification

To capture images, fish were anesthetized with tricaine, and images were taken using fluorescence microscopy (M205FA, Leica) or confocal microscopy (LSM780, Carl Zeiss). For confocal 3D imaging, the fish fins or embryos were embedded in 1.5% low melting temperature agarose gel and observed under a 40X water-immersion objective lens. Assessment of cell location was performed on the reconstructed z-stack images (ZEN software, Carl Zeiss).

## 2.7. Adult caudal fin amputation

The adult fish (> 3-month-old) were used for studying wound repair and skin regeneration. After anesthesia, fish caudal fins were cut by a disinfected scalpel. The cutting plane is set at 1/3 of the vertical midline from the distal site. Fish were returned to the 28.5ºC water system after amputation. Time-laps images were taken at the interval time points during regeneration.

## 2.8. Cryosection

The collected tissue samples were immersed in 4% PFA/PBS solution at 4ºC overnight. Then, the samples were washed with PBT for 5 min (3 times), and gradually dehydrated by 25%, 50%, 75%, and 100% MeOH for 5 min in each step and stored at -30ºC. After gradual rehydration by PBT, the samples were immersed in the 20% sucrose/PBS at 4ºC overnight. Then the samples were put in a drop of O.C.T compound (Tissue-Tek) to remove the surface solution and transferred into a small box made of aluminum foil which fulfilled with O.C.T compound. Then the samples were frozen in liquid nitrogen and stored at -30ºC for at least 2 hours. The completely frozen samples were used for making 12-14 μm thick cryosections by a cryostat at -20ºC.

## 2.9. Fluorescence-activated cell-sorting

The mCherry$^{+}$ or EGFP$^{+}$ cells were isolated from *Tgs* using the fluorescence-activated cell sorter SH800S (SONY) according to the standard protocol (Manoli and Driever, 2012). Briefly, 500–1000 deyolked embryos (Link et al., 2006), or two fins were digested in 0.5% collagenase in PBS at 37 °C for 40 min. The cell suspension was filtered through a strainer (40 μm mesh size, Greiner Bio-One) into the L-15 buffer (1.5 % Leibovitz's L-15, 50 U/mL penicillin, 10 % BSA). After dissociation, the cells were stained with RedDot2 (Biotium) for excluding dead cells during sorting.

## 2.10. RNA extraction

The sorted living cells were directly collected in a lysis buffer and used for RNA extraction using an RNeasy Plus Micro Kit (Qiagen). RNA quality assessment was performed using a 2100 Bioanalyzer (Agilent Technologies). High-quality RNA samples (RIN > 7) were used for RNA sequencing.

## 2.11. RNA sequencing

RNA sequencing was performed at the Seibutsu-Giken Bioengineering Lab (Kanagawa, Japan) on the DNBSEQ-G400 instrument (MGI Tech). High-quality reads were mapped to the zebrafish reference genome sequence (*Danio rerio* GRCz11) using Hisat2 ver.2.1.0 and counted using featureCounts ver. 2.0.3.

## 2.12. DEGs screening and Gene Ontology analysis

The differentially expressed genes (DEGs) (Fig. 21A) were identified according to the following criteria: transcripts per million (TPM) ratio (*itgb4*$^{+}$ cells at 1 dpf vs. *krt4*$^{+}$ cells at 1 dpf) ≥ 5, either of TPM values in *krt4*$^{+}$ cells or *itgb4*$^{+}$ cells ≥ 10. Heatmaps of the DEGs were plotted using EXCEL 2013.

The selected DEGs were used to perform Gene Ontology (GO) analysis using the DAVID Bioinformatics Resource (https://david.ncifcrf.gov) (Huang et al., 2009; Sherman et al., 2022) and mapped with the Gene Ontology database. Enriched terms were ranked according to the number of enriched genes.

## 2.13. Cell ablation

To specifically ablate the *krt4*$^{+}$ keratinocytes or *itgb4*$^{+}$ basal cells in the adult epidermis, 5 mM metronidazole (Mtz, Tokyo Chemical Industry) was dissolved in fish water (0.3% artificial sea salt and 0.0001% methylene blue) and treated with *Tg(krt4:tagBFP-nfsB)* for 4 hrs or the *Tg (itgb4:tagBFP-nfsB)* for 3 hrs for each time. Mtz treatment was repeated every 2 days to increase cell ablation without causing fish death.

## 2.14. AO staining

To evaluate cell ablation efficiency, Acridine orange (AO; Sigma-Aldrich) staining was performed (Tucker and Lardelli, 2007). After Mtz treatment, the fish were placed in 10 μg/mL AO solution for 5 min at room temperature in the dark and washed with fresh water for 3 hrs. After staining, fish were anesthetized with tricaine and observed under a microscope.

## 2.15. Immunostaining and histological analysis

The collected tissues were fixed in 4% PFA overnight at 4 °C and washed with PBTx (0.1% Tween 20, 0.1% TritonX-100 in PBS) 3 times for 5 min. For whole-mount staining, samples were stained with DAPI (1:1000; Dojin Chemical) or SYTO11 (1:500; Thermo Fisher) for staining the nucleus. The cryosections were stained with an anti-EGFP antibody (1:1000; Nacalai Tesque) for 90 min and an anti-rat secondary antibody with Alexa Fluor 488 (1:1000; Thermo Fisher) for 90 min. After 3 times PBTx washing, the samples were

mounted in 80% glycerol containing 2.5 mg/mL DABCO (1, 4-diazabicyclo [2.2. 2] octane) as an antifade reagent and observed by confocal microscopy.

## 2.16. Quantification and statistical analysis

No statistical method was used to determine the sample size. Sample sizes were chosen based on previous publications, and experiment types are shown in the figure legends. After selecting embryos or fish with WT morphology, the clutch mates were randomized into different groups for each experiment. No animal or sample was excluded from the analysis unless the animal died during the procedure. Most assessments of phenotypes and expression patterns were repeated in at least three independent experiments, except for cell sorting and RNA sequencing analyses (two or one replicate). Whenever possible, blinding was performed during data collection and analysis. In some experiments, when blinding was not possible, the same investigator processed the samples and collected data. Sample sizes are indicated in the figures or legends.

Statistical analyses of the quantified data were performed using Microsoft Excel 2013 and GraphPad Prism 6. All statistical values are presented as the mean ± standard error of the mean (s.e.m.).

# Chapter 3 Results

## 3.1. The *itgb4* and *krt18* are selected as markers for epidermal basal cells

To identify markers for basal cells, even in uninjured tissues, we examined previous RNA profiling data and known gene expression patterns (Yoshinari et al., 2009; DeWard et al., 2014; Wehner et al., 2014) and focused on *itgb4* and *krt18*. ISH analysis showed that *itgb4* expression was uniform in the basal layer of the epidermis of both uncut and cut fins (Fig. 11A, C). Unlike *itgb4*, *krt18* was not detected in the epidermis of the uncut fin but was strongly induced by fin amputation in the WE, including the basal cells (Fig. 11B, D).

## 3.2. New Cre-*Tgs* were established with *itgb4* and *krt18* promoters

Using the promoters of *itgb4* and *krt18,* we generated transgenic lines (*Tgs*) expressing the CreERt2 fusion protein (Fig. 12A, B). When the respective lines were crossed with the RSG-Cre reporter *Tg* (Yoshinari et al., 2012), and recombination with 4-OH tamoxifen (TAM) was induced, $EGFP^{+}$ cells appeared in the WE of the *krt18:creERt2* line and the basal cells of the uncut *itgb4:creERt2* line (Fig. 12C, D).

## 3.3. Embryonic epidermal cells become heterogeneous by 24 hpf

Embryonic development and homeostasis in adult tissues have been investigated independently. However, how embryonic cells give rise to adult tissues is not well understood. We sought to determine when basal stem cell progenitors emerge during development.

We performed ISH analysis for *krt4,* a gene expressed in keratinocytes (Chen et al., 2011), *krt18*, and *itgb4* during embryonic development (Fig. 13A). Both *krt18* and *krt4* were uniformly expressed in epithelial cells at 50% epiboly stage. At the somite stage and thereafter, *krt18* expression was downregulated and nearly disappeared from epithelial cells by 24 hours post fertilization (hpf), whereas *krt4* expression persisted in a subset of epithelial cells. In contrast to *krt18* and *krt4*, *itgb4* expression became evident only after 24 hpf. ISH analysis using *krt4* and *krt18* probes together showed that a population of *krt4*$^{-}$*/krt18*$^{-}$ epithelial cells were present (Fig. 13B), indicating that embryonic epithelial cells became heterogeneous by 24 hpf.

## 3.4. Strong *krt18* expression is only detected in the early embryonic stage, whereas the *itgb4* expression is started in the later stage.

To further determine the expression of marker genes during embryonic development, I established a series of reporter *Tgs*: *Tg(krt4:tagBFP-nfsB), Tg(itgb4:mcherry),* and *Tg(krt18:mcherry)*. From the observation from double *Tg(krt4:tagBFP-nfsB; krt18:mcherry)*, the mcherry of *krt18* was strongly expressed by 1 dpf, but gradually become weaker at 2 dpf and mostly undetectable at 3 dpf (Fig 14). Also, I generated double *Tg(krt4:tagBFP-nfsB; itgb4:mcherry)* to find the earliest stage that the *itgb4* is started expressed. The mcherry of *itgb4* was undetectable in the early stage until 21 hpf (Fig. 15). These data showed a consistent result in the ISH experiment.

## 3.5. Identities of heterogeneous epidermal cells at 1 dpf by transgenic lines

In order to know the precise distribution of heterogeneous epidermal cells, the analyses of confocal 3D images and cryosections showed that *krt18*$^{+}$ or *krt4*$^{+}$ cells were confined to the periderm at 24 hpf (upper layer of the epidermis; Le Guellec et al., 2004; Shibata et al., 2018), in which there are four types of heterogeneous epithelial cells, *krt4*$^{+}$/*krt18*$^{+}$ (75.3%), *krt4*$^{+}$/*krt18*$^{-}$ (9.7%), *krt4*$^{-}$/*krt18*$^{+}$ (7.7%), *krt4*$^{-}$ /*krt18*$^{-}$ (7.3%) (Fig. 16A, B). At 3 dpf, the *krt4*$^{+}$/*krt18*$^{-}$ cells became predominant in the periderm (96.8%) (Fig. 16B, C), whereas *itgb4*$^{+}$ cells were observed in the deeper layers (Fig. 16A, C). Together, these observations suggest that *krt4*$^{+}$/*krt18*$^{+}$ embryonic epithelial cells become heterogeneous at the somite stage and that *itgb4*$^{+}$ deeper cells are generated from a fraction of epithelial cells in which *keratin* gene expression is downregulated.

## 3.6. The *itgb4*$^{+}$ cells at 1 dpf are the origin of adult basal stem cells

To reveal the origin of basal stem cells, we used the *krt4, krt18,* or *itgb4* promoters in Cre *Tgs* and tracked cell fate from embryonic stages. When labeling with *krt4:cre* or *krt18:cre* was performed at the pre-somite stage (TAM 0-10 hpf), EGFP$^{+}$ cells gave rise to the epidermal cells of the larvae and adult fish (Fig. 17A). When labeling was performed at the somite stage (TAM 10-24 hpf) or later stage (TAM 1-2 dpf), EGFP$^{+}$ cells labeled with *krt4:cre* or *krt18:cre* were observed in the larval epidermis but their progenies disappeared from the epidermis without contributing to the adult epidermis (Fig. 17B, C), indicating that they are transient cells that are not maintained until the adult stage.

In contrast to *krt4:cre* and *krt18:cre, itgb4:cre*-labeled cells contributed to the adult epidermis including the basal stem cells (Fig. 17C), and were maintained throughout life which producing keratinocytes (Fig. 18), although labeled cells were also observed in the larval epidermis as in the *krt4:cre* and *krt18:cre* lines. By time-lapse tracing, the *itgb4*-labeled cells at 1 dpf gradually increased in the epidermis and occupied over 90% of the epidermal cells by 42 dpf, whereas the *krt4:cre*-labeled cells decreased in inverse proportion (Fig. 19). By such transition, embryonic epithelial cells were disposed of and replaced with stem cell-derived keratinocytes.

## 3.7. Identity of basal stem cells is evident immediately after fate segregation

Thus, lineage tracing suggested that basal cell fate segregation occurs during the somite stage. Next, we investigated whether the identity of the basal cells was evident after fate segregation. To this end, the *krt4*$^{+}$ cells were isolated from 1 dpf embryos of *Tg(krt4:creERt2;RSG)* that were treated with TAM for 10-24 hpf (Fig. 20A). This was done to precisely sort the cells that expressed *krt4* during 10-24 hpf stage. And the *itgb4*$^{+}$ cells were isolated by fluorescence-activated cell sorting from 1 dpf embryos and adult caudal fins of *Tg(itgb4:mcherry)* (Fig. 20 B, C).

By comparing the enriched transcripts in *krt4*$^{+}$ and *itgb4*$^{+}$ cells at 1 dpf, we identified 147 enriched genes in *itgb4*$^{+}$ cells and 381 enriched genes in *krt4*$^{+}$ cells (Fig. 21A). Among the *itgb4*$^{+}$ cell-enriched genes, as many as 57% (83 genes) also showed apparent expression in the adult basal cells (Fig. 21A). GO analysis showed that these

genes are characteristic of the basal cell functions, such as focal adhesion, cell-matrix adhesion, and integrin binding (Ghorbani et al., 2022) (Fig. 21B), whereas many of the *krt4*$^{+}$ cell-enriched genes that showed a low expression both in the embryonic and adult *itgb4*$^{+}$ cells (86%, 328 genes) had functions in cell junctions, cell differentiation, and oxidoreductase activity (Piao et al., 2011) (Fig. 21C). Together, these data suggest that *itgb4*$^{+}$ cells already possess a basal cell identity immediately after fate segregation.

## 3.8. Basal cells actively proliferate with three patterns in juvenile skin

Next, we investigated the behavior of basal progenitors during fish growth and homeostasis. As Cre labeling by TAM produced too many EGFP$^{+}$ cells to track individual cells (Fig. 22A-C), we used the estrogen receptor antagonist, fulvestrant (ICI-182780, termed ICI hereafter) to sparsely label the *itgb4*$^{+}$ basal cells of the epidermis (Shibata et al., 2018) and tracked their fates (Fig. 22B, C).

We first labeled *itgb4*$^{+}$ cells at the juvenile stage (Ribas and Piferrer, 2014) and tracked cell fate. Cell behavior was categorized into three proliferation patterns: fast-proliferating (more than two cell divisions, 29.2%), slow-proliferating (one or two cell division, 35.3%), and quiescent (no cell division, 35.5%) (Fig. 23A–D). Confocal optical sections showed that fast-proliferating clones were composed of non-basal cells, whereas slow-proliferating and quiescent clones contained only basal cells (Fig. 23B, D). We also performed long-term cell tracking for three months and observed that many of the fast-proliferating clones finally disappeared from the epidermis (Fig. 24A, B), suggesting that in many cases, the fast clones did not have basal cells, that is, the basal cells differentiated

without retaining the basal cells (Jones and Watt, 1993; Suzuki and Senoo, 2012). Importantly, clones composed of only basal cells were either slow-proliferating self-renewing clones or quiescent basal stem cells (Fig. 23B; Fig. 24C, D). Taken together, it can be concluded that many *itgb4*$^{+}$ basal cells of juvenile fish are active in producing both more basal cells and differentiated keratinocytes.

## 3.9. Basal cells become quiescent in the mature epidermis

In contrast to the juvenile stage, as many as 70.5% of labeled basal cells were quiescent, and only 3.5% were fast-proliferating within a two-week time window in adult fish (> 3-month-old) (Fig. 25A–C), indicating that many of basal cells become quiescent and rarely differentiate into the TACs in the adult epidermis. During the long-term tracking, the slow-proliferating clones gradually expanded over time, producing more basal cells (Fig. 26A, B).

## 3.10. Activation of quiescent basal stem cells by fin amputation

We investigated the regulation of quiescent basal cells to renew and/or differentiate into TAC/keratinocytes in response to tissue injury. We first analyzed basal cell behavior during fin regeneration.

As observed by Shibata et al. (2018), the basal cells closest to the amputation site disappeared rapidly (Fig. 27A). Basal cells in the adjacent region were highly proliferative and rapidly expanded in size (Fig. 27A). These large clones (> 20 cells) contained both basal cells and differentiating keratinocytes (Fig. 27B), indicating that basal cell renewal

and differentiation occurred nearby. In the proximal region, quiescent or slowly proliferating (self-renewing) clones were dominant. Distinct signals are speculated to induce basal cell self-renewal and differentiation.

## 3.11. Basal cell differentiation is induced by *krt4*$^{+}$ keratinocyte ablation

Next, we investigated how basal cell renewal and differentiation are regulated in response to injury. To do this, we injured keratinocytes or basal stem cells using *Tgs* expressing the nitroreductase, *nfsB* (Ando et al., 2017), under the control of *krt4* or *itgb4* promoters. The basal cells were labeled 4 days before ablation, and Mtz treatment was repeated at 2-day intervals (Fig. 29A). The apoptosis of the respective cells was successfully induced without causing fish death (Fig. 28A, B).

Upon injury to *krt4*$^{+}$ non-basal cells, differentiation of basal cells into non-basal cells and rapid proliferation were induced (Fig. 29B, C). However, basal cell self-renewal was rarely observed.

## 3.12. Basal cell self-renewal is induced by *itgb4*$^{+}$ basal cell ablation through re-expressing *krt18.*

In contrast to non-basal injury, basal cell injury induced basal cell self-renewal, whereas basal cell differentiation was rarely observed (Fig. 30A, B). These results indicate that injuries to non-basal keratinocytes or basal cells cause different signals for basal cells to adopt either self-renewal or differentiation.

We further showed that *krt18* expression was induced by injury to basal cells but not to non-basal keratinocytes (Fig. 31). We labeled and tracked the fate of *krt18*$^{+}$ cells using *Tg(krt18:creERt2),* in which the *krt18*$^{+}$ basal cells were labeled at 1 day after basal cell injury (Fig. 32A). Tracking revealed that most of the *krt18*-expressed cells (88%, n = 66 out of 75 clones) self-renewed to produce basal cells (Fig. 32B), indicating that basal cell self-renewal proceeds through the *krt18*$^{+}$ state, and that *krt18* expression may represent a de-differentiated status of basal cells.

# Chapter 4 Discussion

To perform a comprehensive analysis of basal cells during development, growth, and homeostasis, we established new *Tgs* with *itgb4* and *krt18* promoters to label epidermal basal cells and studied their fate and behavior. In this study, we revealed that the basal cells are derived from the *itgb4*$^{+}$ embryonic epithelial cells at the somite stage. These cells proliferate to increase in number and produce TACs to generate keratinocytes, which finally expel embryonic epithelial cells. Although basal stem cells became mostly quiescent in adult fish, we revealed that injuries to keratinocytes or basal cells induce different basal cell reactions, differentiation into TACs, or basal cell self-renewal, respectively (Fig. 33).

## 4.1. The *itgb4* and *krt18* as markers for epidermal basal cells

In this study, we adopted *itgb4* and *krt18* as basal cell markers. *itgb4* is a subunit of the Integrin α6β4, which is a component of hemidesmosomes that plays essential roles in strengthening and stabilizing the skin (Wilhelmsen et al., 2006). *itgb4* is highly expressed in the epithelial stem cells of the adult esophagus in mice (DeWard et al., 2014). The *krt18* is a type I intermediate filament protein expressed in basal epidermal cells of zebrafish fins during regeneration (Wehner et al., 2014; Jacob et al., 2018).

Several studies have used *p63* and *krtt1c19e* as epidermal basal cell markers (Guzman et al., 2013; Lee et al., 2014; Chen et al., 2016). However, both *p63* and *krtt1c19e* have also been detected in the suprabasal cells of the adult epidermis (Guzman et al., 2013; Lee et al., 2014). Our ISH analysis and *Cre*-labeling experiments identified that *itgb4* is

specifically expressed in the basal layer of the epidermis throughout life, whereas *krt18* is only induced in regenerating basal cells. Because of the specific localization of *itgb4* and *krt18* to basal cells, these genes and *Tgs* are useful tools for investigating basal cell behavior in homeostatic and regenerative situations.

## 4.2. Origin of the basal cells at the somite stage

Little is known about how embryonic cells give rise to adult tissues in many organs. In the case of the epidermis, a previous study using *Tg(krtt1c19e:cre)* in zebrafish reported that *krtt1c19e*$^{+}$ basal cells labeled at 72-73.5 hpf contributed to the adult epidermis, suggesting that these larval cells include the basal cell progenitors (Lee et al., 2014).

In this study, we showed that cell fate decisions occur as early as the somite stage before epidermal stratification in a population of embryonic epithelial cells. What mechanisms induce fate determination in basal stem cells? Possible explanations include induction signals from tissues or cells, or that they occur stochastically. This issue remains a subject for future research.

Mechanisms underlying epidermal stratification are intriguing. Some studies in mice have suggested that asymmetric division of the basal cells that produce differentiating suprabasal cells drives stratification (Lechler and Fuchs, 2005; Damen et al., 2021). However, in this study, we did not observe the asymmetric division of basal cells before 7 dpf (Fig. 19), although epidermal stratification began at 1 dpf (Fig. 16C). The asymmetric division may not be the primary driving force of epidermal stratification. A study using zebrafish suggested that E-cadherin and aPKC have a polarized distribution in the bi-

layered epidermis and regulate the polarity of basal cells and the periderm (Arora et al., 2020). Changes in cell identity and expression of adhesion molecules can regulate epidermal stratification from an early stage.

## 4.3. Conserved mechanism of epidermal homeostasis between zebrafish and mammals

Lineage tracing of individual basal cells suggested that *itgb4*$^{+}$ cells actively proliferate in juvenile fish, in which they adopt three different cell behavior patterns: fast-proliferating, slow-proliferating, and quiescent. These observations are consistent with previous studies in mice (Clayton et al., 2007; Li and Clevers, 2010; Damen et al., 2021; Koren et al., 2022). Thus, our study in zebrafish demonstrates that the overall structure and behavior of basal stem cells are strikingly conserved between fish and mammals. Taking advantage of tissue transparency and live imaging, zebrafish serves as a useful model for revealing the regulatory mechanisms of self-renewal and differentiation of basal stem cells (Pan et al., 2013).

## 4.4. Injuries to different cell types induce differential responses in basal cells

In this study, we revealed that self-renewal or differentiation of basal cells is induced by injury to different cell types. This finding suggests that different signals originating from different cells regulate the response of basal cells. Moreover, we showed that the *krt18* was re-expressed in basal cells undergoing self-renewal. *krt18* is highly expressed in gastric

cancer cells and promotes cell proliferation and migration (Wang et al., 2021). It is speculated that *krt18* could be a marker of dedifferentiated basal cells that acquire a proliferative status.

Studies in mice have suggested that the self-renewal of basal cells is driven by the differentiation of neighboring basal cells (Mesa et al., 2018). Furthermore, it has been suggested that cell signaling pathways such as Delta-Notch (Lowell et al., 2000) and BMP-FGF (Zhu et al., 2014) are essential for controlling the self-renewal and differentiation of epidermal basal cells. Brock et al. (2019) suggested that dead basal cells release *wnt8a* into the apoptotic bodies to stimulate epidermal cell proliferation. Moreover, Horsley et al. (2008) have shown that Nfatc1 balances the quiescence and proliferation of skin stem cells. Such molecules and/or signals could be mediators from non-basal keratinocytes or surrounding basal cells that regulate the basal cell response to injuries. However, further studies are required to reveal the implicated signals and their crosstalk.

# Chapter 5 Reference


**Ando, K., Shibata, E., Hans, S., Brand, M. and Kawakami, A.** (2017). Osteoblast Production by Reserved Progenitor Cells in Zebrafish Bone Regeneration and Maintenance. *Dev Cell* **43**, 643-650.e3.

**Arora, P., Dongre, S., Raman, R. and Sonawane, M.** (2020). Stepwise polarisation of developing bilayered epidermis is mediated by aPKC and E-cadherin in zebrafish. *Elife* **9**, e49064.

**Bakkers, J., Hild, M., Kramer, C., Furutani-Seiki, M. and Hammerschmidt, M.** (2002). Zebrafish ΔNp63 is a direct target of Bmp signaling and encodes a transcriptional repressor blocking neural specification in the ventral ectoderm. *Developmental cell* **2**, 617-627.

**Barbieri, J., Wanat, K. and Seykora, J.** (2014). Skin: basic structure and function. *Pathobiology of Human Disease*, 1134-1144.

**Benitah, S. A. and Frye, M.** (2012). Stem cells in ectodermal development. *Journal of molecular medicine* **90**, 783-790.

**Blanpain, C. and Fuchs, E.** (2009). Epidermal homeostasis: a balancing act of stem cells in the skin. *Nature reviews Molecular cell biology* **10**, 207-217.

**Blanpain, C., Lowry, W. E., Pasolli, H. A. and Fuchs, E.** (2006). Canonical notch signaling functions as a commitment switch in the epidermal lineage. *Genes & development* **20**, 3022-3035.

**Brocard, J., Warot, X., Wendling, O., Messaddeq, N., Vonesch, J.-L., Chambon, P. and Metzger, D.** (1997). Spatio-temporally controlled site-specific somatic mutagenesis in the mouse. *Proceedings of the National Academy of Sciences* **94**, 14559-14563.

**Brock, C. K., Wallin, S. T., Ruiz, O. E., Samms, K. M., Mandal, A., Sumner, E. A. and Eisenhoffer, G. T.** (2019). Stem cell proliferation is induced by apoptotic bodies from dying cells during epithelial tissue maintenance. *Nature Communication* **10**, 1044.

**Buch, T., Heppner, F. L., Tertilt, C., Heinen, T. J., Kremer, M., Wunderlich, F. T., Jung, S. and Waisman, A.** (2005). A Cre-inducible diphtheria toxin receptor mediates cell lineage ablation after toxin administration. *Nature methods* **2**, 419-426.

**Chang, W. J. and Hwang, P. P.** (2011). Development of zebrafish epidermis. *Birth Defects Research* **93**, 205-214.

**Chen, C.-F., Chu, C.-Y., Chen, T.-H., Lee, S.-J., Shen, C.-N. and Hsiao, C.-D.** (2011). Establishment of a transgenic zebrafish line for superficial skin ablation and functional validation of apoptosis modulators in vivo. *PLoS One* **6**, e20654.

**Chen, C.-H., Puliafito, A., Cox, B. D., Primo, L., Fang, Y., Di Talia, S. and Poss, K. D.** (2016). Multicolor cell barcoding technology for long-term surveillance of epithelial regeneration in zebrafish. *Dev Cell* **36**, 668-680.

**Cheung, T. H. and Rando, T. A.** (2013). Molecular regulation of stem cell quiescence. *Nature reviews Molecular cell biology* **14**, 329-340.

**Clayton, E., Doupé, D. P., Klein, A. M., Winton, D. J., Simons, B. D. and Jones, P. H.** (2007). A single type of progenitor cell maintains normal epidermis. *Nature* **446**, 185-189.

**Curado, S., Anderson, R. M., Jungblut, B., Mumm, J., Schroeter, E. and Stainier, D. Y.** (2007). Conditional targeted cell ablation in zebrafish: a new tool for regeneration studies. *Developmental dynamics: an official publication of the American Association of Anatomists* **236**, 1025-1035.

**Damen, M., Wirtz, L., Soroka, E., Khatif, H., Kukat, C., Simons, B. D. and Bazzi, H.** (2021). High proliferation and delamination during skin epidermal stratification. *Nat Commun* **12**, 3227.

**DeWard, A. D., Cramer, J. and Lagasse, E.** (2014). Cellular heterogeneity in the mouse esophagus implicates the presence of a nonquiescent epithelial stem cell population. *Cell Reports* **9**, 701-711.

**Feil, R., Wagner, J., Metzger, D. and Chambon, P.** (1997). Regulation of Cre recombinase activity by mutated estrogen receptor ligand-binding domains. *Biochemical and biophysical research communications* **237**, 752-757.

**Fuchs, E.** (2008). Skin stem cells: rising to the surface. *The Journal of cell biology* **180**, 273-284.

**Gahtan, E. and Baier, H.** (2004). Of lasers, mutants, and see‐through brains: Functional neuroanatomy in zebrafish. *Journal of neurobiology* **59**, 147-161.

**Gaspard, N. and Vanderhaeghen, P.** (2010). Mechanisms of neural specification from embryonic stem cells. *Current opinion in neurobiology* **20**, 37-43.

**Ghahary, A., Shen, Y. J., Nedelec, B., Wang, R., Scott, P. G. and Tredget, E. E.** (1996). Collagenase production is lower in post-burn hypertrophic scar fibroblasts than in normal fibroblasts and is reduced by insulin-like growth factor-1. *Journal of Investigative Dermatology* **106**, 476-481.

**Ghorbani, S., Shahrokhtash, A., Gautrot, J. E. and Sutherland, D. S.** (2022). Protein ligand nanopattern size selects for cellular adhesion via hemidesmosomes over focal adhesions. *Small Methods* **6**, 2200152.

**Goodell, M. A., Nguyen, H. and Shroyer, N.** (2015). Somatic stem cell heterogeneity: diversity in the blood, skin and intestinal stem cell compartments. *Nature reviews Molecular cell biology* **16**, 299-309.

**Grohmann, M., Paulmann, N., Fleischhauer, S., Vowinckel, J., Priller, J. and Walther, D. J.** (2009). A mammalianized synthetic nitroreductase gene for high-level expression. *BMC cancer* **9**, 1-12.

**Gu, H., Zou, Y.-R. and Rajewsky, K.** (1993). Independent control of immunoglobulin switch recombination at individual switch regions evidenced through Cre-loxP-mediated gene targeting. *Cell* **73**, 1155-1164.

**Guzman, A., Ramos-Balderas, J. L., Carrillo-Rosas, S. and Maldonado, E.** (2013). A stem cell proliferation burst forms new layers of P63 expressing suprabasal cells during zebrafish postembryonic epidermal development. *Biology Open* **2**, 1179-1186.

**Han, D. D., Stein, D. and Stevens, L. M.** (2000). Investigating the function of follicular subpopulations during Drosophila oogenesis through hormone-dependent enhancer-targeted cell ablation. *Development* **127**, 573-583.

**Hardman, M. J., Sisi, P., Banbury, D. N. and Byrne, C.** (1998). Patterned acquisition of skin barrier function during development. *Development* **125**, 1541-1552.

**Hayashi, S. and McMahon, A. P.** (2002). Efficient recombination in diverse tissues by a tamoxifen-inducible form of Cre: a tool for temporally regulated gene activation/inactivation in the mouse. *Developmental biology* **244**, 305-318.

**Henrikson, R. C. and Gedeon Matoltsy, A.** (1967a). The fine structure of teleost epidermis: I. Introduction and filament-containing cells. *Journal of Ultrastructure Research* **21**, 194-212.

**Henrikson, R. C. and Gedeon Matoltsy, A.** (1967b). The fine structure of teleost epidermis: II. Mucous cells. *Journal of Ultrastructure Research* **21**, 213-221.

**Henrikson, R. C. and Gedeon Matoltsy, A.** (1967c). The fine structure of teleost epidermis: III. Club cells and other cell types. *Journal of Ultrastructure Research* **21**, 222-232.

**Horsley, V., Aliprantis, A. O., Polak, L., Glimcher, L. H. and Fuchs, E.** (2008). NFATc1 balances quiescence and proliferation of skin stem cells. *Cell* **132**, 299-310.

**Horsley, V., O'Carroll, D., Tooze, R., Ohinata, Y., Saitou, M., Obukhanych, T., Nussenzweig, M., Tarakhovsky, A. and Fuchs, E.** (2006). Blimp1 defines a progenitor population that governs cellular input to the sebaceous gland. *Cell* **126**, 597-609.

**Hou, Y., Lee, H. J., Chen, Y., Ge, J., Osman, F. O. I., McAdow, A. R., Mokalled, M. H., Johnson, S. L., Zhao, G. and Wang, T.** (2020). Cellular diversity of the regenerating caudal fin. *Science Advances* **6**, eaba2084.

**Huang, D. W., Sherman, B. T. and Lempicki, R. A.** (2009). Systematic and integrative analysis of large gene lists using DAVID bioinformatics resources. *Nature protocols* **4**, 44-57.

**Indra, A. K., Warot, X., Brocard, J., Bornert, J.-M., Xiao, J.-H., Chambon, P. and Metzger, D.** (1999). Temporally-controlled site-specific mutagenesis in the basal layer of the epidermis: comparison of the recombinase activity of the tamoxifen-inducible Cre-ERT and Cre-ERT2 recombinases. *Nucleic acids research* **27**, 4324-4327.

**Ito, M., Liu, Y., Yang, Z., Nguyen, J., Liang, F., Morris, R. J. and Cotsarelis, G.** (2005). Stem cells in the hair follicle bulge contribute to wound repair but not to homeostasis of the epidermis. *Nature medicine* **11**, 1351-1354.

**Jacob, J. T., Coulombe, P. A., Kwan, R. and Omary, M. B.** (2018). Types I and II keratin intermediate filaments. *Cold Spring Harbor Perspectives in Biology* **10**, a018275.

**Jones, P. H. and Watt, F. M.** (1993). Separation of human epidermal stem cells from transit amplifying cells on the basis of differences in integrin function and expression. *Cell* **73**, 713-724.

**Karttunen, M. J. and Lyons, D. A.** (2019). A drug-inducible transgenic zebrafish model for myelinating glial cell ablation. *Oligodendrocytes: Methods and Protocols*, 227-238.

**Kawakami, A.** (2010). Stem cell system in tissue regeneration in fish. *Dev Growth Differ* **52**, 77-87.

**Kawakami, A., Fukazawa, T. and Takeda, H.** (2004). Early fin primordia of zebrafish larvae regenerate by a similar growth control mechanism with adult regeneration. *Developmental dynamics: an official publication of the American Association of Anatomists* **231**, 693-699.

**Kimmel, C. B., Warga, R. M. and Schilling, T. F.** (1990). Origin and organization of the zebrafish fate map. *Development* **108**, 581-594.

**Koren, E., Feldman, A., Yusupova, M., Kadosh, A., Sedov, E., Ankawa, R., Yosefzon, Y., Nasser, W., Gerstberger, S. and Kimel, L. B.** (2022). Thy1 marks a distinct population of slow-cycling stem cells in the mouse epidermis. *Nature Communication* **13**, 4628.

**Kos, C. H.** (2004). Methods in nutrition science: Cre/loxP system for generating tissue-specific knockout mouse models. *Nutrition reviews* **62**, 243-246.

**Koster, M. I. and Roop, D. R.** (2004). The role of p63 in development and differentiation of the epidermis: Tanioku kihei memorial lecture. *Journal of dermatological science* **34**, 3-9.

**Le Guellec, D., Morvan-Dubois, G. and Sire, J.-Y.** (2003). Skin development in bony fish with particular emphasis on collagen deposition in the dermis of the zebrafish (Danio rerio). *International Journal of Developmental Biology* **48**, 217-231.

**Le Guellec, D., Morvan-Dubois, G. and Sire, J.-Y.** (2004). Skin development in bony fish with particular emphasis on collagen deposition in the dermis of the zebrafish (Danio rerio). *International Journal of Developmental Biology* **48**, 217-231.

**Lechler, T. and Fuchs, E.** (2005). Asymmetric cell divisions promote stratification and differentiation of mammalian skin. *Nature* **437**, 275-280.

**Lee, R. T., Asharani, P. and Carney, T. J.** (2014). Basal keratinocytes contribute to all strata of the adult zebrafish epidermis. *PLoS One* **9**, e84858.

**Li, L. and Clevers, H.** (2010). Coexistence of quiescent and active adult stem cells in mammals. *science* **327**, 542-545.

**Lindmark, D. G. and Müller, M.** (1976). Antitrichomonad action, mutagenicity, and reduction of metronidazole and other nitroimidazoles. *Antimicrobial agents and chemotherapy* **10**, 476-482.

**Link, V., Shevchenko, A. and Heisenberg, C.-P.** (2006). Proteomics of early zebrafish embryos. *BMC Developmental Biology* **6**, 1-9.

**Lowell, S., Jones, P., Le Roux, I., Dunne, J. and Watt, F. M.** (2000). Stimulation of human epidermal differentiation by Delta–Notch signalling at the boundaries of stem-cell clusters. *Current Biology* **10**, 491-500.

**Manoli, M. and Driever, W.** (2012). Fluorescence-activated cell sorting (FACS) of fluorescently tagged cells from zebrafish larvae for RNA isolation. *Cold Spring Harbor Protocols* **2012**, pdb. prot069633.

**Mascré, G., Dekoninck, S., Drogat, B., Youssef, K. K., Brohée, S., Sotiropoulou, P. A., Simons, B. D. and Blanpain, C.** (2012). Distinct contribution of stem and progenitor cells to epidermal maintenance. *Nature* **489**, 257-262.

**Mesa, K. R., Kawaguchi, K., Cockburn, K., Gonzalez, D., Boucher, J., Xin, T., Klein, A. M. and Greco, V.** (2018). Homeostatic epidermal stem cell self-renewal is driven by local differentiation. *Cell Stem Cell* **23**, 677-686. e4.

**Niezgoda, A., Niezgoda, P., Nowowiejska, L., Białecka, A., Męcińska-Jundziłł, K., Adamska, U. and Czajkowski, R.** (2017). Properties of skin stem cells and their potential clinical applications in modern dermatology. *European Journal of Dermatology* **27**, 227-236.

**O'Brien, G. S., Rieger, S., Wang, F., Smolen, G. A., Gonzalez, R. E., Buchanan, J. and Sagasti, A.** (2012). Coordinate development of skin cells and cutaneous sensory axons in zebrafish. *Journal of Comparative Neurology* **520**, 816-831.

**Opalenik, S. R. and Davidson, J. M.** (2005). Fibroblast differentiation of bone marrow‐derived cells during wound repair. *The FASEB Journal* **19**, 1561-1563.

**Orford, K. W. and Scadden, D. T.** (2008). Deconstructing stem cell self-renewal: genetic insights into cell-cycle regulation. *Nature Reviews Genetics* **9**, 115-128.

**Page, M. E., Lombard, P., Ng, F., Göttgens, B. and Jensen, K. B.** (2013). The epidermis comprises autonomous compartments maintained by distinct stem cell populations. *Cell stem cell* **13**, 471-482.

**Pan, Y. A., Freundlich, T., Weissman, T. A., Schoppik, D., Wang, X. C., Zimmerman, S., Ciruna, B., Sanes, J. R., Lichtman, J. W. and Schier, A. F.** (2013). Zebrabow: multispectral cell labeling for cell tracing and lineage analysis in zebrafish. *Development* **140**, 2835-2846.

**Piao, M. S., Choi, J.-Y., Lee, D.-H., Yun, S. J., Lee, J.-B. and Lee, S.-C.** (2011). Differentiation-dependent expression of NADP (H): quinone oxidoreductase-1 via NF-E2 related factor-2 activation in human epidermal keratinocytes. *Journal of dermatological science* **62**, 147-153.

**Poss, K. D., Shen, J., Nechiporuk, A., McMahon, G., Thisse, B., Thisse, C. and Keating, M. T.** (2000). Roles for Fgf signaling during zebrafish fin regeneration. *Developmental biology* **222**, 347-358.

**Potten, C. S., Schofield, R. and Lajtha, L. G.** (1979). A comparison of cell replacement in bone marrow, testis and three regions of surface epithelium. *Biochimica et Biophysica Acta (BBA)-Reviews on Cancer* **560**, 281-299.

**Pourghadamyari, H., Rezaei, M., Ipakchi-Azimi, A., Eisa-Beygi, S., Basiri, M., Tahamtani, Y. and Baharvand, H.** (2019). Establishing a new animal model for muscle regeneration studies. *Molecular Biology Research Communications* **8**, 171.

**Rawlings, A. and Harding, C.** (2004). Moisturization and skin barrier function. *Dermatologic therapy* **17**, 43-48.

**Ribas, L. and Piferrer, F.** (2014). The zebrafish (D anio rerio) as a model organism, with emphasis on applications for finfish aquaculture research. *Reviews in Aquaculture* **6**, 209-240.

**Rompolas, P., Mesa, K. R. and Greco, V.** (2013). Spatial organization within a niche as a determinant of stem-cell fate. *Nature* **502**, 513-518.

**Sauer, B. and Henderson, N.** (1988). Site-specific DNA recombination in mammalian cells by the Cre recombinase of bacteriophage P1. *Proceedings of the National Academy of Sciences* **85**, 5166-5170.

**Sherman, B. T., Hao, M., Qiu, J., Jiao, X., Baseler, M. W., Lane, H. C., Imamichi, T. and Chang, W.** (2022). DAVID: a web server for functional enrichment analysis and functional annotation of gene lists (2021 update). *Nucleic Acids Res* **50**, W216-W221.

**Shibata, E., Ando, K., Murase, E. and Kawakami, A.** (2018). Heterogeneous fates and dynamic rearrangement of regenerative epidermis-derived cells during zebrafish fin regeneration. *Development* **145**, dev162016.

**Smart, I.** (1970). Variation in the plane of cell cleavage during the process of stratification in the mouse epidermis. *British Journal of Dermatology* **82**, 276-282.

**Snippert, H. J., Haegebarth, A., Kasper, M., Jaks, V., van Es, J. H., Barker, N., van de Wetering, M., van den Born, M., Begthel, H. and Vries, R. G.** (2010). Lgr6 marks stem cells in the hair follicle that generate all cell lineages of the skin. *Science* **327**, 1385-1389.

**Sternberg, N. and Hamilton, D.** (1981). Bacteriophage P1 site-specific recombination: I. Recombination between loxP sites. *Journal of molecular biology* **150**, 467-486.

**Suzuki, D. and Senoo, M.** (2012). Increased p63 phosphorylation marks early transition of epidermal stem cells to progenitors. *The Journal of Investigative Dermatology* **132**, 2461.

**Tan, Y. R., Liaw, M. and Chen, C.-H.** (2023). The hidden depths of zebrafish skin. *Elife* **12**, e88597.

**Thisse, C. and Thisse, B.** (2008). High-resolution in situ hybridization to whole-mount zebrafish embryos. *Nature Protocols* **3**, 59-69.

**Tucker, B. and Lardelli, M.** (2007). A rapid apoptosis assay measuring relative acridine orange fluorescence in zebrafish embryos. *Zebrafish* **4**, 113-116.

**Wang, P. B., Chen, Y., Ding, G. R., Du, H. W. and Fan, H. Y.** (2021). Keratin 18 induces proliferation, migration, and invasion in gastric cancer via the MAPK signalling pathway. *Clinical and Experimental Pharmacology and Physiology* **48**, 147-156.

**Wehner, D., Cizelsky, W., Vasudevaro, M. D., Özhan, G., Haase, C., Kagermeier-Schenk, B., Röder, A., Dorsky, R. I., Moro, E. and Argenton, F.** (2014). Wnt/β-catenin signaling defines

organizing centers that orchestrate growth and differentiation of the regenerating zebrafish caudal fin. *Cell Reports* **6**, 467-481.

**Wickett, R. R. and Visscher, M. O.** (2006). Structure and function of the epidermal barrier. *American journal of infection control* **34**, S98-S110.

**Wilhelmsen, K., Litjens, S. H. and Sonnenberg, A.** (2006). Multiple functions of the integrin α6β4 in epidermal homeostasis and tumorigenesis. *Mol Cell Biol* **26**, 2877-2886.

**Wilson, P. A. and Hemmati-Brivanlou, A.** (1995). Induction of epidermis and inhibition of neural fate by Bmp-4. *Nature* **376**, 331-333.

**Wilson, S., Rydström, A., Trimborn, T., Willert, K., Nusse, R., Jessell, T. M. and Edlund, T.** (2001). The status of Wnt signalling regulates neural and epidermal fates in the chick embryo. *Nature* **411**, 325-330.

**Woodley, D. T., Chen, J. D., Kim, J. P., Sarret, Y., Iwasaki, T., Kim, Y. H. and O'Keefe, E. J.** (1993). Re-epithelialization: human keratinocyte locomotion. *Dermatologic Clinics* **11**, 641-646.

**Yoshinari, N., Ando, K., Kudo, A., Kinoshita, M. and Kawakami, A.** (2012). Colored medaka and zebrafish: transgenics with ubiquitous and strong transgene expression driven by the medaka beta-actin promoter. *Dev Growth Differ* **54**, 818-28.

**Yoshinari, N., Ishida, T., Kudo, A. and Kawakami, A.** (2009). Gene expression and functional analysis of zebrafish larval fin fold regeneration. *Developmental Biology* **325**, 71-81.

**Yoshinari, N. and Kawakami, A.** (2011). Mature and juvenile tissue models of regeneration in small fish species. *The Biological Bulletin* **221**, 62-78.

**Yousef, H., Alhajj, M. and Sharma, S.** (2022). Anatomy, skin (integument), epidermis. Treasure Island (FL): StatPearls Publishing.

**Zhu, X.-J., Liu, Y., Dai, Z.-M., Zhang, X., Yang, X., Li, Y., Qiu, M., Fu, J., Hsu, W. and Chen, Y.** (2014). BMP-FGF signaling axis mediates Wnt-induced epidermal stratification in developing mammalian skin. *PLoS Genetics* **10**, e1004687.

# Chapter 6 Acknowledgements

In this study, I appreciate Professor Hiroshi Kimura and Doctor Yuko Satoh at Tokyo Institute of Technology, Kimura Lab. for providing the FACS machine (SONY SH800S) and the helpful guidance. I also appreciate the Open Research Facilities for Life Science and Technology in Tokyo Inst. Technology for providing confocal microscopy (LSM 780) and DNA sequencing. Besides, I appreciate the Seibutsu-Giken Bioengineering Lab (Kanagawa, Japan) for performing RNA sequencing.

I sincerely appreciate my academic supervisor, Dr. Atsushi Kawakami for guiding my daily research and encouraging me to always positively face the difficulties and the challenges during studying life. And thanks to Yidan Meng and Ayu Ishikura for their cooperation in my research project. I would also like to appreciate Dr. Eri Shibata, Dr. Kazunori Ando, and Dr. Siyu Zhou for helping me quickly adapted to the research life. Moreover, I am very grateful to all members who are studying in the Kawakami lab at Tokyo Inst. Technology. Their warm care and help left me with an unforgettable memory in Japan.

Lastly, I sincerely appreciate my parents for their financial support and spiritual encouragement.

# Chapter 7 Figures

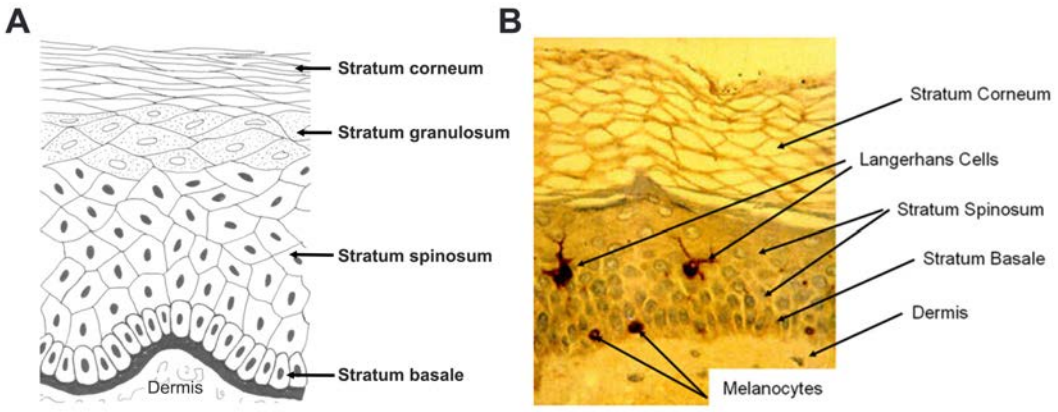


## Fig. 1. Structure of the mammalian epidermis

(A) Illustration of the structure of the mammalian epidermis.

(B) Section of the mammalian epidermis. Many types of epidermis cells distribute in the different epidermal layers. The Langerhans cells are localized in the stratum spinosum and the melanocytes are limited in the stratum basale.

The figure is quoted from Wickett and Visscher (2006).

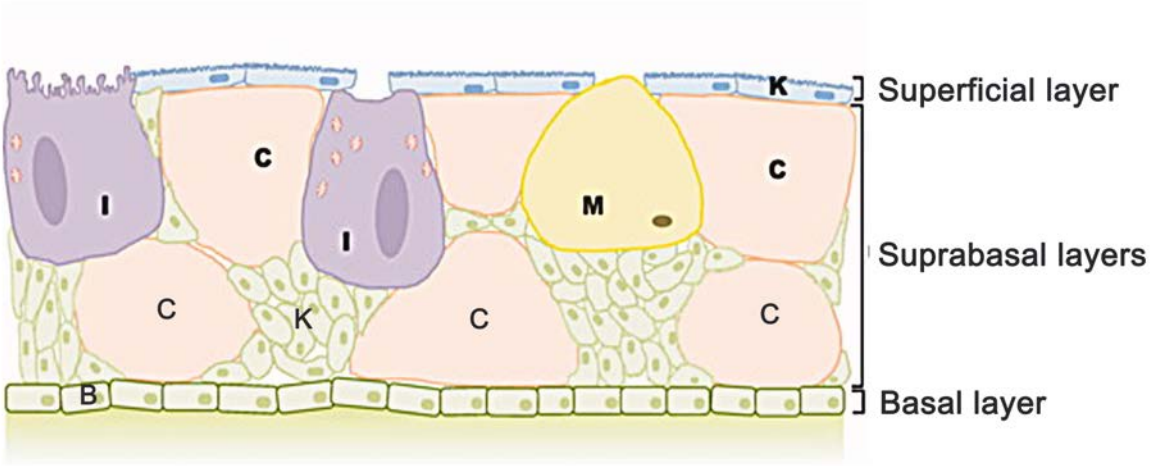


## Fig. 2. Structure of the adult zebrafish epidermis

Scheme of adult zebrafish epidermis. The epidermis is composed of superficial, suprabasal, and basal layers. Keratinocytes (K), superficial and suprabasal layers. Club cells (C), suprabasal layer. Ionocytes (I), suprabasal layer. Mucous cells (M), suprabasal layer. Basal cells (B), basal layer. The epidermal stem cells are localized in the basal layer.
The figure is quoted from Chang and Hwang (2011).

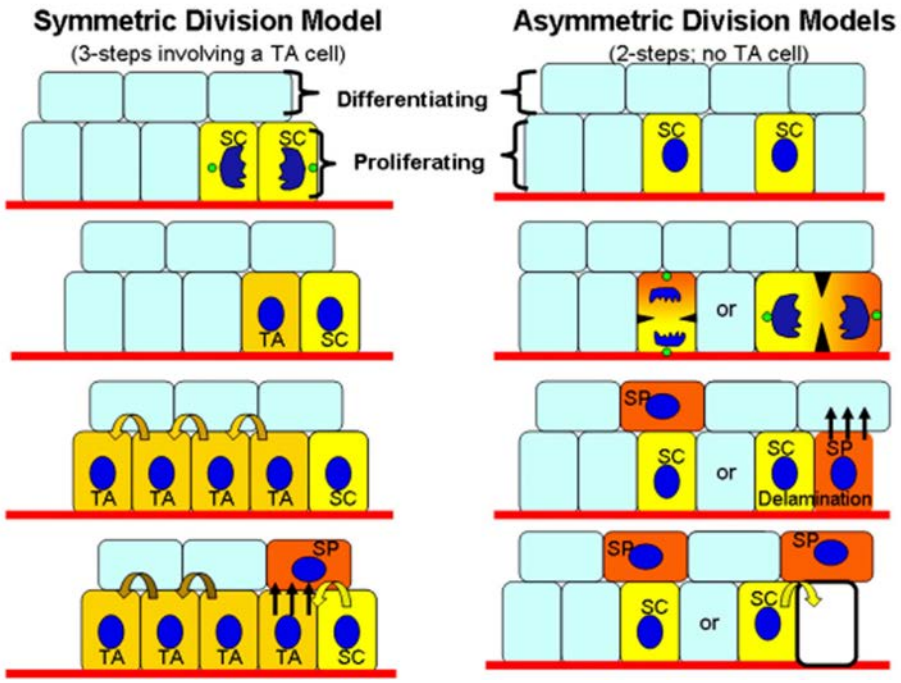


**Fig. 3. Epidermal basal cells undergo both symmetric and asymmetric division**

In the mammalian epidermis, both symmetric and asymmetric divisions are orchestrated during homeostasis. In the symmetric division, a basal stem cell commits to two TACs, and the TACs delaminated from the basal layer to become suprabasal keratinocytes. In asymmetric division, a stem cell divides into a stem cell and a suprabasal cell along with either perpendicular or lateral orientation.

This figure is quoted from Fuchs (2008).

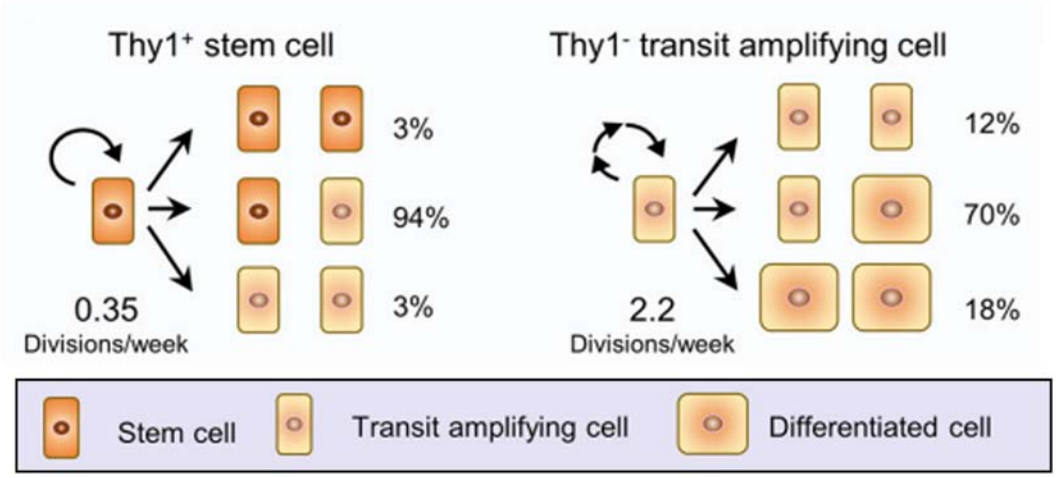


**Fig. 4. The *thy1*$^{+}$ stem cells occasionally produce the fast-cycling TACs during homeostasis**

During epidermal turnover in the mouse model, the slow-cycling *thy1*$^{+}$ basal stem cells undergo both asymmetric and symmetric division to produce new stem cells or TACs. And the TACs actively proliferate to become terminally differentiated keratinocytes. All of the TACs have a disappeared fate in the long run.

This figure is quoted from Koren et al. (2022).

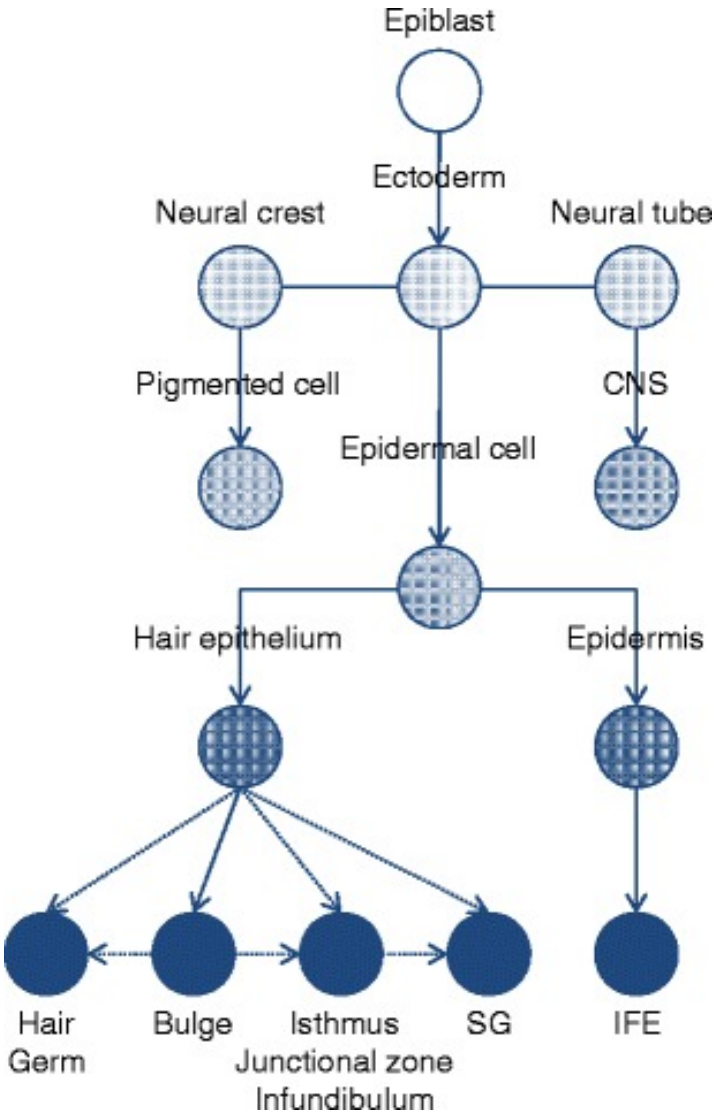


## Fig. 5. Developmental hierarchy for epidermal stem cell population

All the epidermal stem cells are derived from the epiblast at the pre-gastrulation stage. During gastrulation, some of the epiblast cells turn into three germ layers, the ectoderm contributes to all epidermal stem cell lineages. CNS, central nervous system. SG, sebaceous gland. IFE, the interfollicular epidermis.

This figure is quoted from Benitah and Frye (2012).

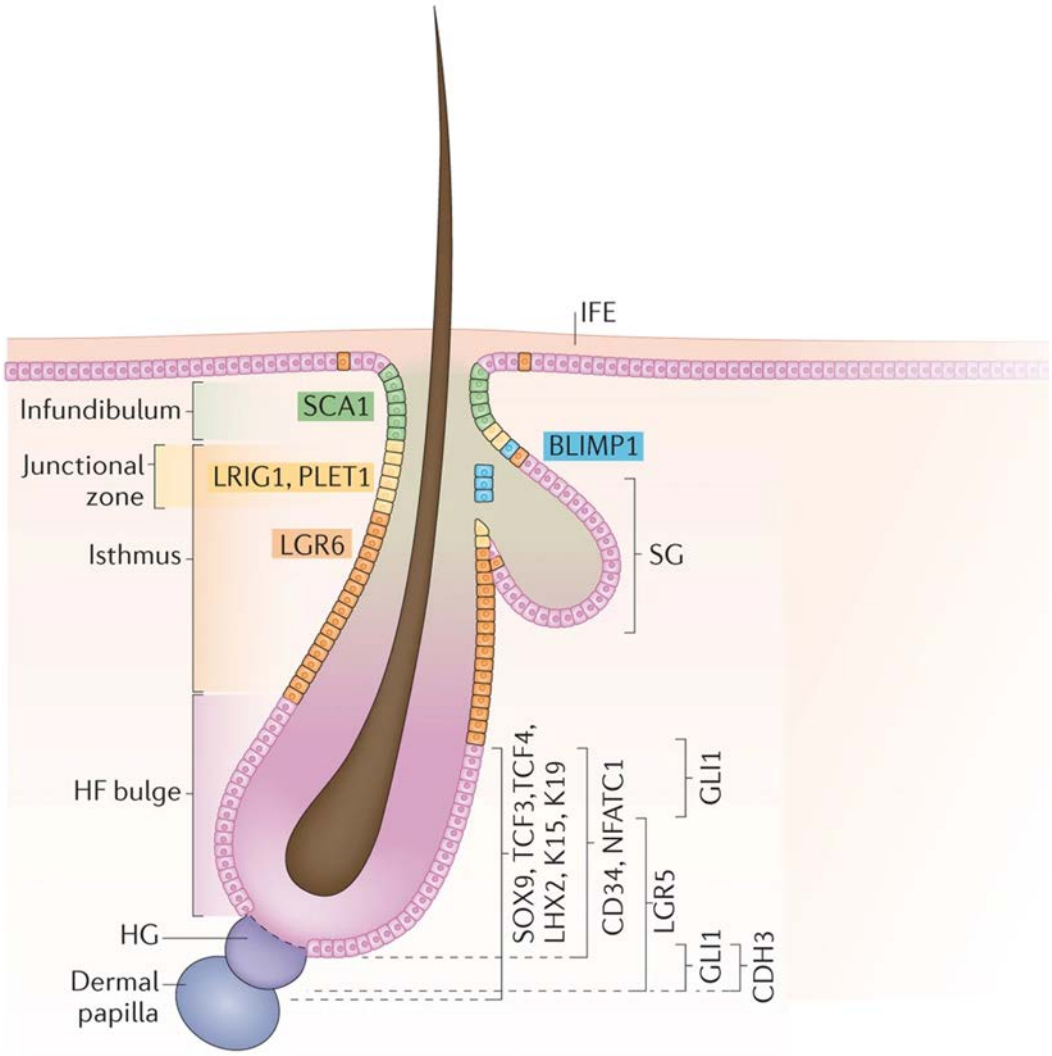


## Fig. 6. Heterogeneity of the basal cells in mammalian epidermis

In the mammalian hair follicle (HF), different populations of stem cells were identified in the basal layers of the epidermis with their marker genes. IFE, the interfollicular epidermis. HG, hair germ. SG, sebaceous gland. These heterogeneous basal cells are distributed in the distinct zones of HF and have restricted lineage potential during normal homeostasis and expanded potential in response to injury.

This figure is quoted from Goodell et al. (2015).

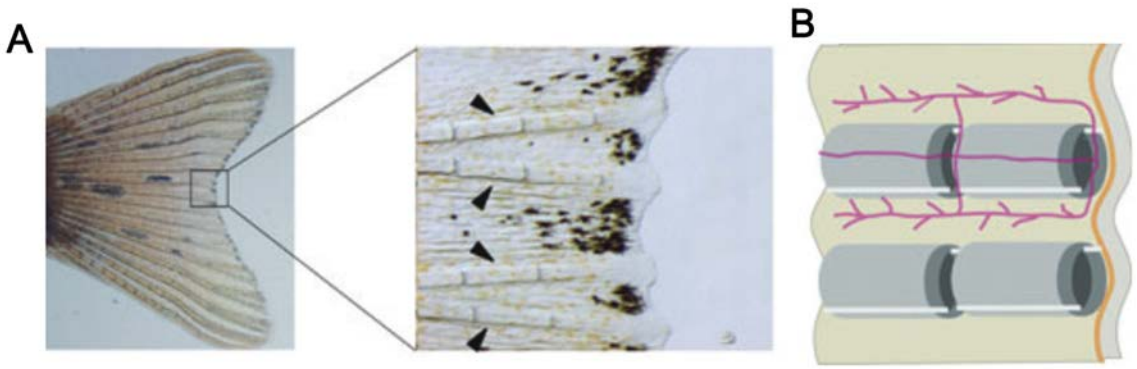


## Fig. 7. Structure of the adult zebrafish fin

(A) Image of an adult zebrafish caudal fin (left panel) and magnification of the boxed area (right panel). The caudal fin consists of the segmented fin-ray bones (arrowheads) which are surrounded by mesenchymal cells and covered with thin epidermis. The randomly distributed black spots are the chromatophores.
(B) Scheme of the structure of the caudal fin. A segment of fin-ray bone is composed of two hemi-rays. The surrounding pink lines represent the blood vessels.
This figure is quoted from Kawakami (2010).

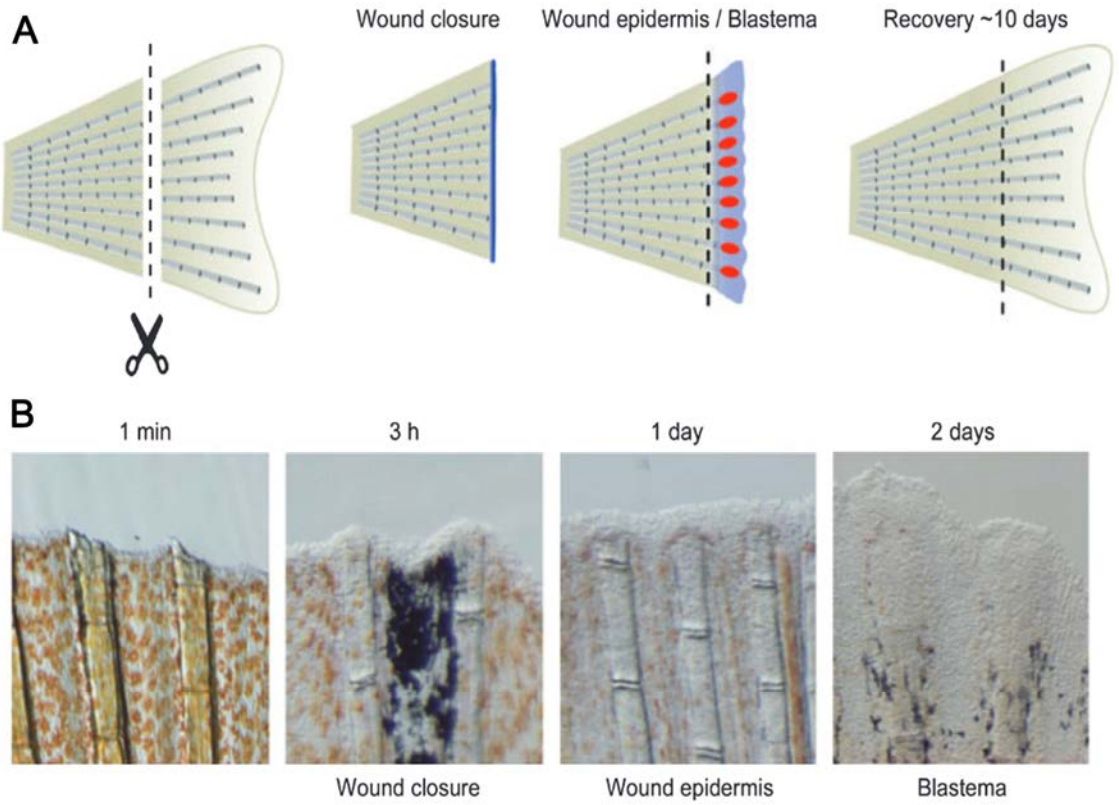


## Fig. 8. Epimorphic regeneration in adult zebrafish fin

(A) Procedure of fin regeneration after amputation. The amputated wound site is sealed by the growing epithelial cells by 3 hpa. At 1 day post amputation (dpa), the wound epidermis and blastema (red ovals) are formed near the wound site. Their proliferation in the excessive period to regrowth the lost tissues until the newly regenerated fin is completed by approximately 10 days with original size.

(B) Time-laps images of regenerating caudal fin. The irregularly distributed golden and black spots are the chromatophores.

This figure is quoted from Kawakami (2010).

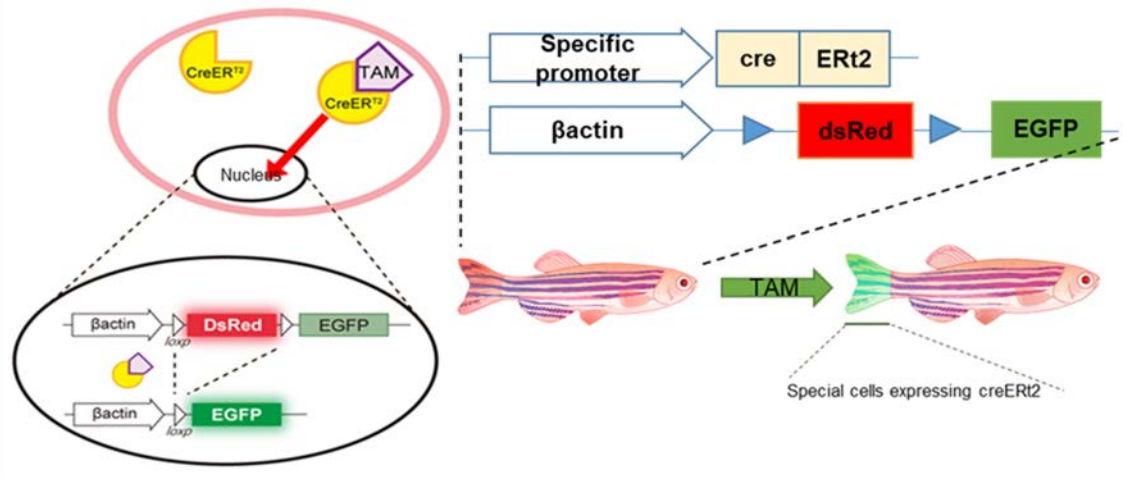


**Fig. 9. The scheme of the Cre-*lox*P system is used to specifically and conditionally label the special cells**

The specific promoter drives the CreERt2 expression in a group of cells. After the treatment with 4-OH tamoxifen (TAM) or fulvestrant (ICI), CreERt2 enters the nucleus and induces the recombination at the *lox*P sites, resulting in switching of the fluorescence from red (Dsred) to green (EGFP).

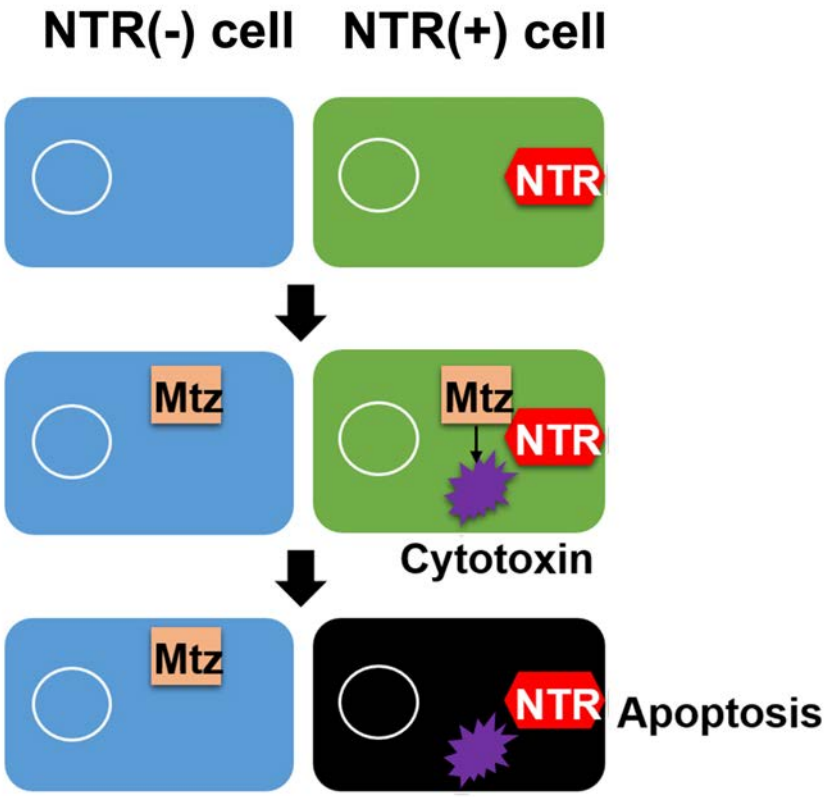


**Fig. 10. Specific cell ablation by NTR-Mtz system**

The NTR-Mtz system is an inducible tool to specifically ablate the target cells. Specific promoter drives the nitroreductase (NTR) protein expression. The NTR converts the non-toxic prodrug Mtz to a cytotoxic DNA cross-linking agent and finally induces cell apoptosis.

This figure is quoted from Ando Kazunori (doctoral thesis, 2017).

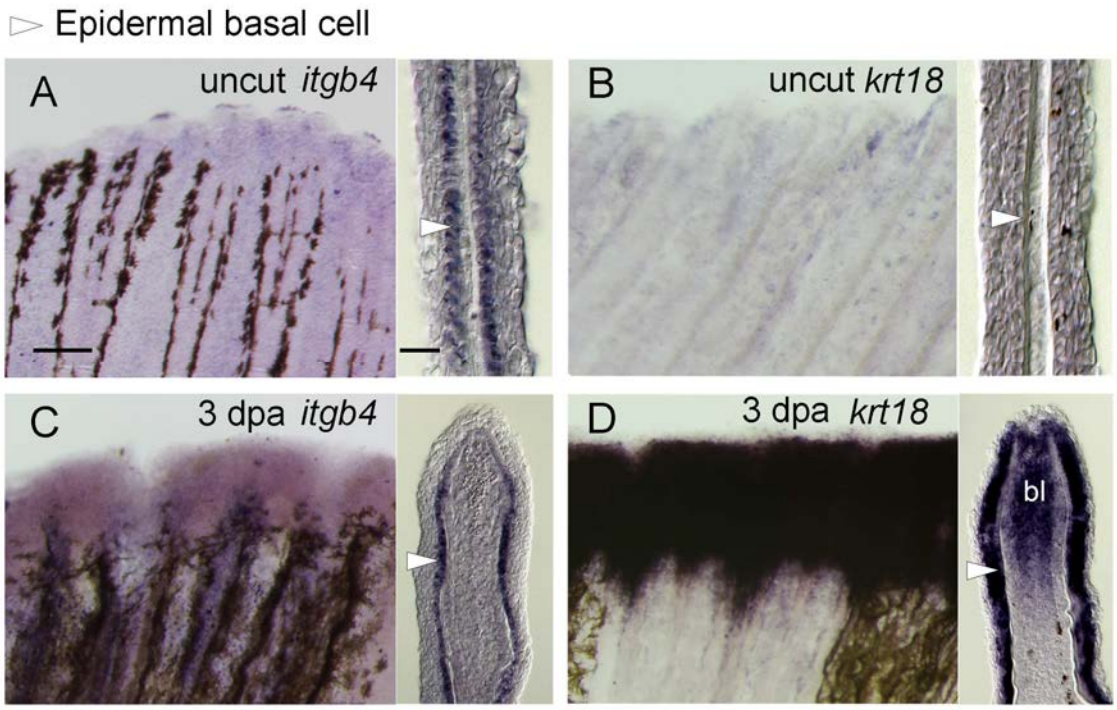


**Fig. 11. ISH of *itgb4* and *krt18* expression in the amputated and natural caudal fin**

Whole-mount *in situ* hybridization (ISH) of *itgb4* and *krt18* genes in adult zebrafish fin. dpa, days post amputation. bl, blastema. Respective longitudinal sections are shown on the right side. *itgb4* is expressed in the basal layer of the amputated and uncut fin, whereas *krt18* is only expressed in the regenerating fin. Arrowheads show the basal layer of the epidermis. Scale bars, 100 μm (whole mount) and 30 μm (section).

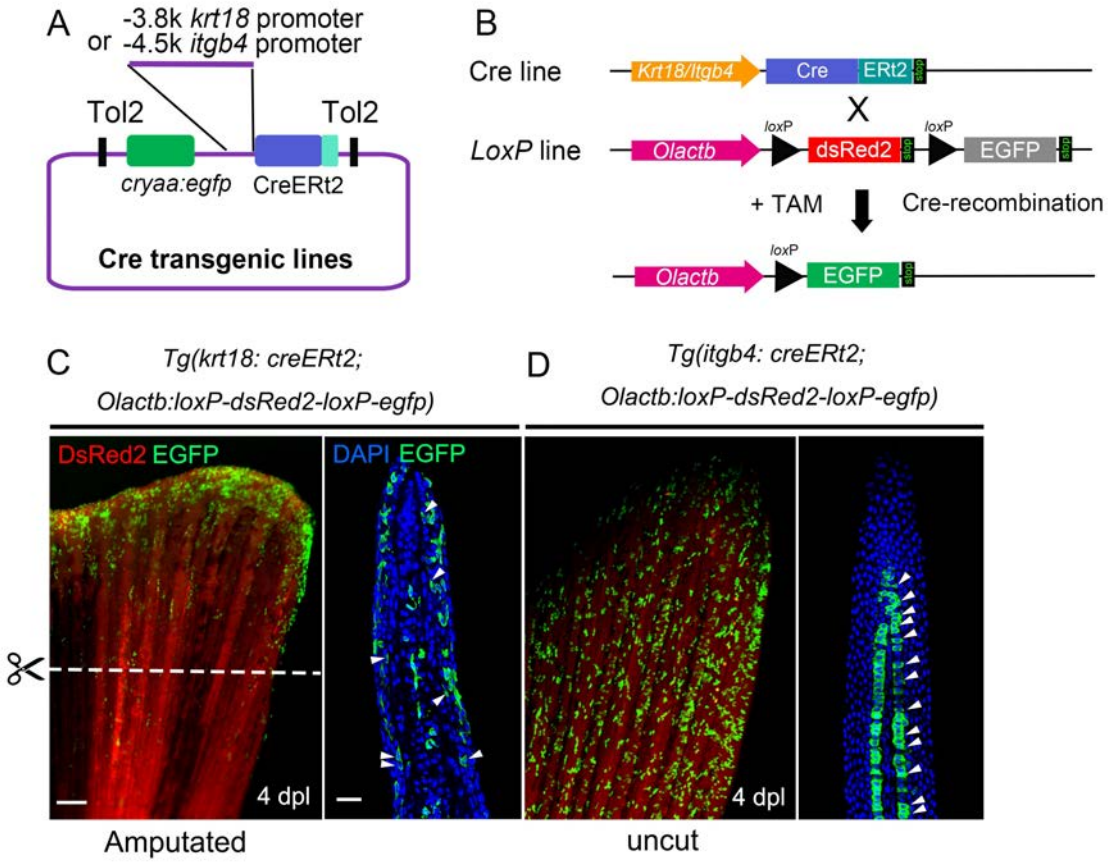


## Fig. 12. Establishment of Cre-*Tgs* with *itgb4* and *krt18* promoters

(A) A diagram of the Tol2 transposon-based vector used to generate the *Tgs. cryaa, crystalline alpha a* promoter.

(B) A scheme illustrating the Cre-mediated lineage tracing. The double *Tgs* of the Cre-expressing line and the *lox*P reporter line were treated with tamoxifen (TAM) or fulvestrant (ICI) to induce the recombination at *lox*P sites. The resulting EGFP expression persists in all progeny cells. pA, polyadenylation signal sequence.

(C, D) EGFP expression in the amputated fin of *Tg(krt18:creERt2)* (C) and uncut fin of *Tg(itgb4:creERt2)* (D). TAM was added at 3 dpa in (C) and images were taken at 4 days post labeling (dpl) in (C, D). Broken line, amputation plane. Dotted line, basement

membrane. Arrowheads, representative EGFP-labeled basal cells, and surface keratinocytes. Scale bars, 300 μm (left) and 50 μm (right).

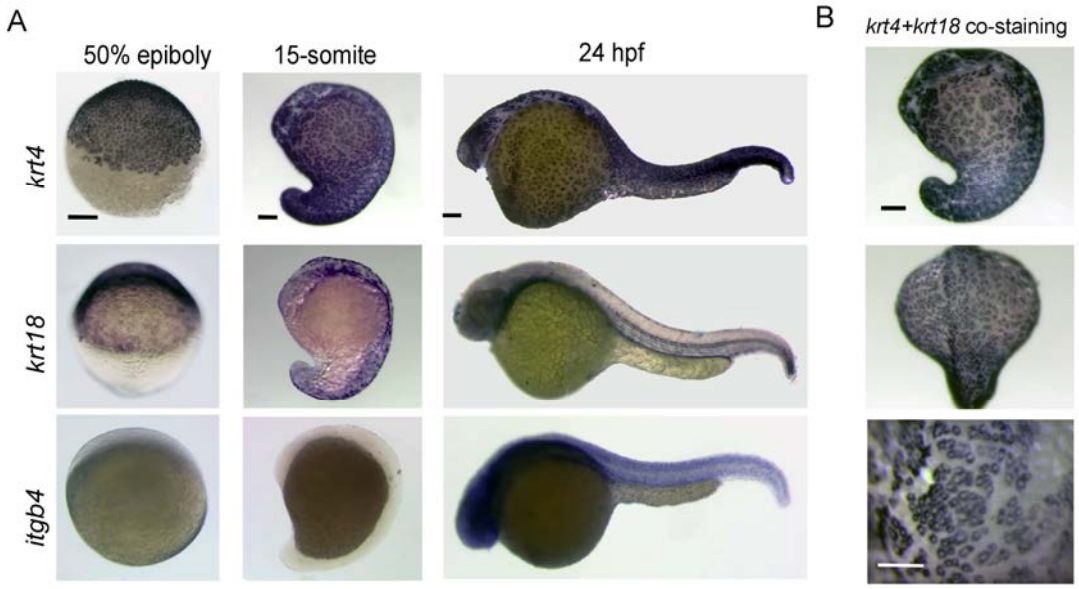


## Fig. 13. ISH of *krt4*, *krt18* and *itgb4* in embryonic stages

(A) ISH analysis of *krt4*, *krt18,* and *itgb4* expression. *krt4* was detected in all embryonic stages. *krt18* is expressed in the early embryonic stage, but the expression declined after 24 hours post fertilization (hpf). *itgb4* was only detected later than 24 hpf. At the somite stage onward, epithelial cells have a mosaic expression of *krt4* and *krt18*. Scale bars, 50 μm for respective stages.

(B) ISH analysis at the 15-somite stage probed with both *krt4* and *krt18*. Embryonic epithelial cells contain the $krt4^{-}/krt18^{-}$ cells. Scale bar, 50 μm.

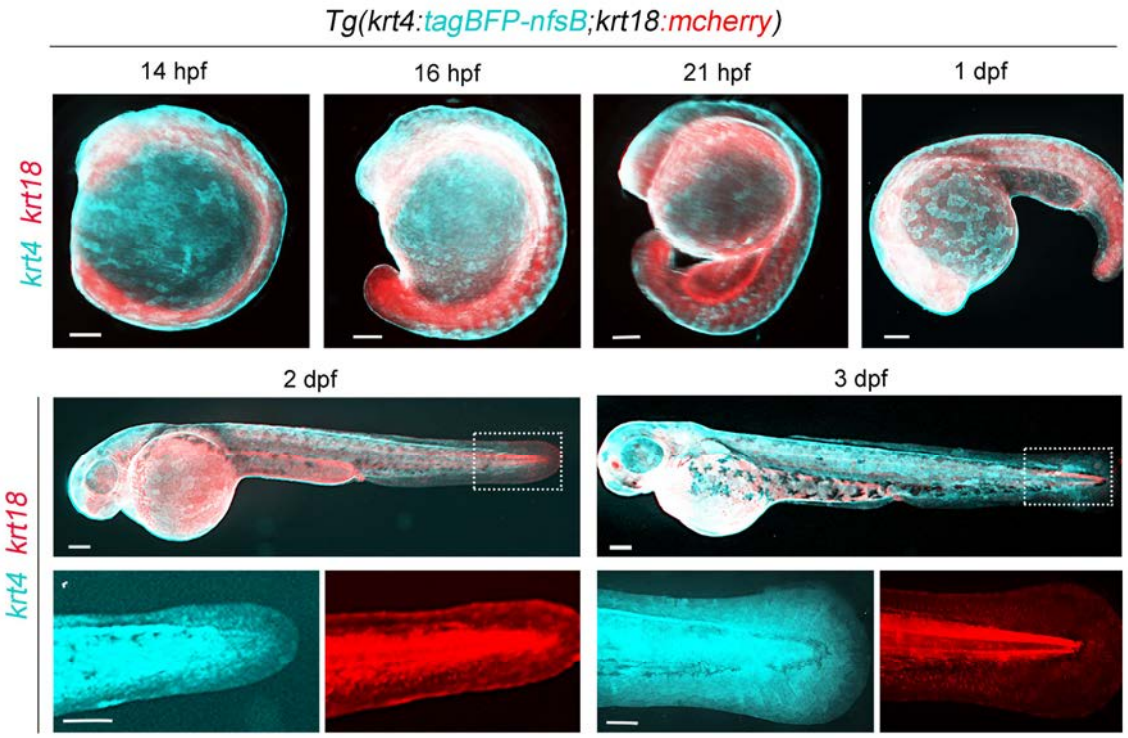


**Fig. 14. Strong expression of *krt18* is only detectable in the early embryonic stage**

Fluorescent microscope time-lapse images of the *Tg(krt4:tagBFP-nfsB;krt18:mcherry)*. The mCherry fluorescence of *krt18* significantly decreased from 2 dpf, while the BFP fluorescent of *krt4* was continuously maintained in the epidermis. Scale bars, 100 μm.

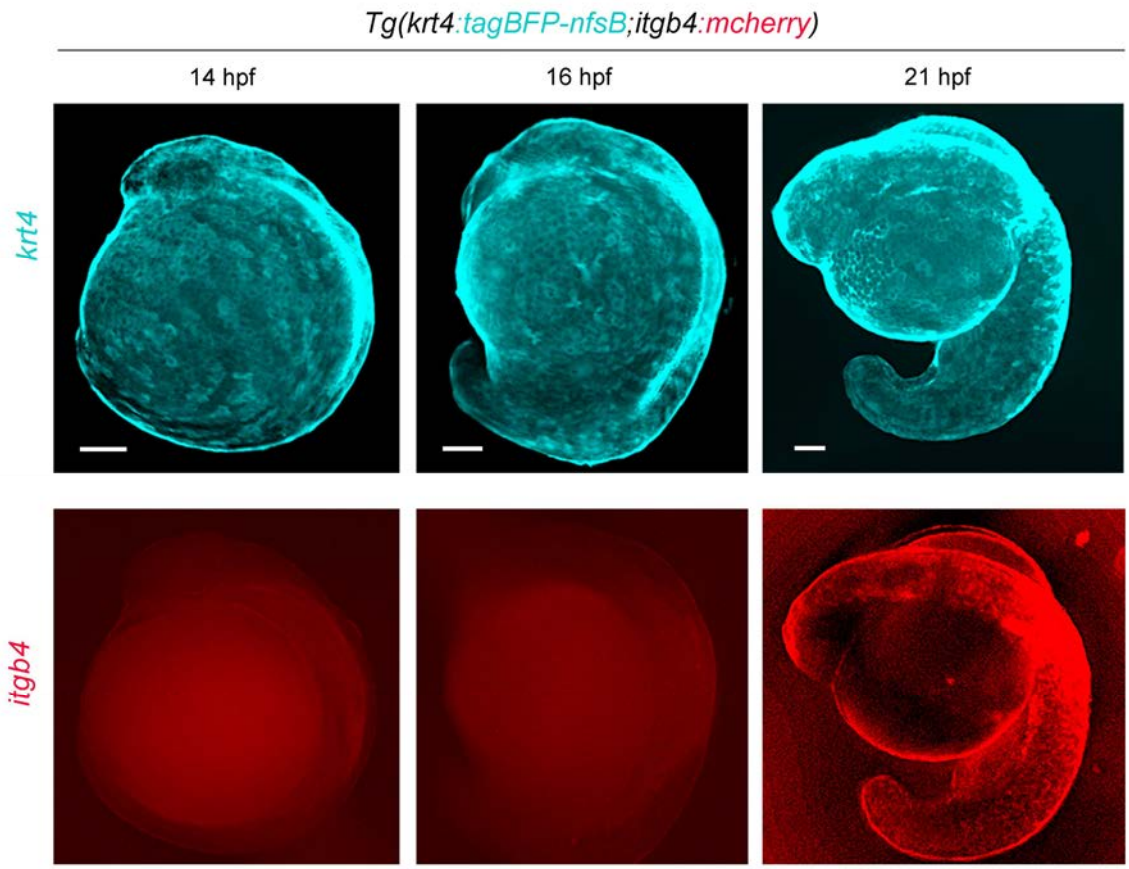


**Fig. 15. The *itgb4* expression is started in the later embryonic stage around 21 hpf**

Fluorescent microscope images of *Tg(krt4:tagBFP-nfsB;itgb4:mcherry)* during embryonic development. *itgb4*$^{+}$ cells were detected after 21 hpf, while *krt4* was continuously expressed in all stages. Scale bars, 100 μm.

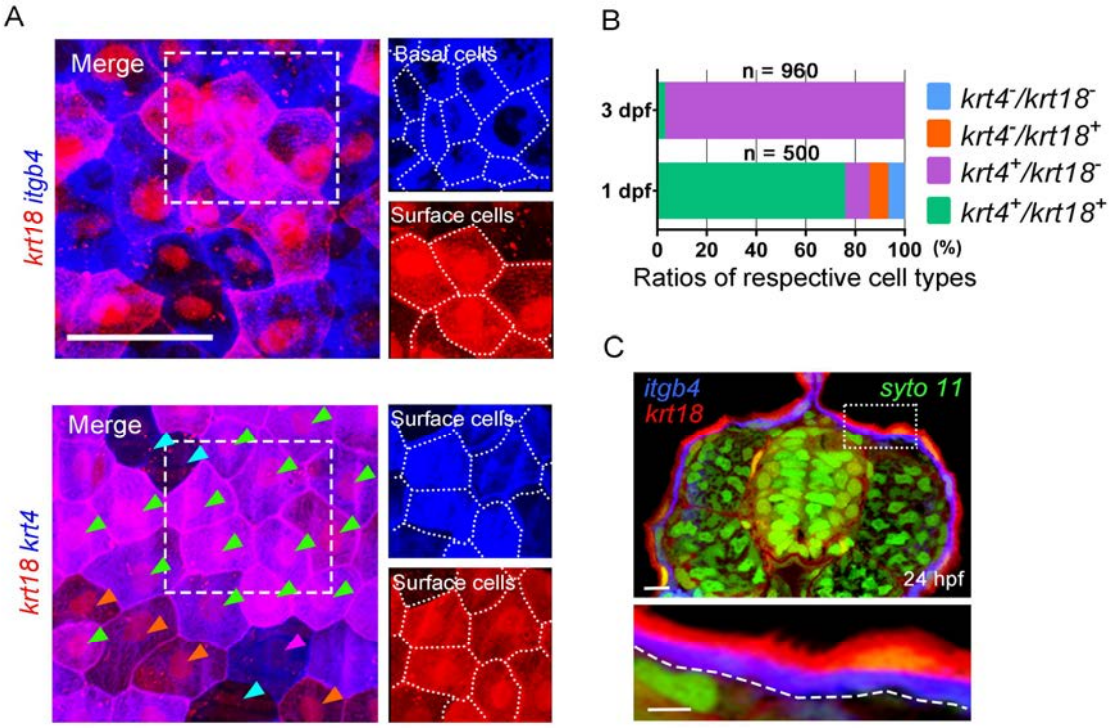


## Fig. 16. Identities of heterogeneous epidermal cells at 1 dpf

(A) Confocal images of epithelial cells of *Tg(krt18:mchery;itgb4:tagBFP-nfsB)* or *Tg(krt18:mcherry;krt4:tagBFP-nfsB)* at 1 dpf. Respective BFP and mCherry channels of the squared regions (broken lines) are shown on the right side. *itgb4* and *krt4* expression (upper panels) was observed in the deeper basal progenitors and surface epithelial cells, respectively. Both *krt4* and *krt18* were observed in the surface epithelial cells (lower panels) but the expression of *krt4* and *krt18* was not uniform. Colored arrowheads indicate

the epithelial cells with different combinations of *krt18* and *krt4* expression (also see d). Dotted lines, the boundary of cells. Scale bar, 20 μm.

(B) Ratios of epithelial cells with different combinations of *krt18* and *krt4* expression at 1dpf and 3 dpf. Note that the ratio of *krt18*$^{+}$ cells decreased at 3 dpf. n = 500 surface cells from 7 embryos (1 dpf) and 960 surface cells from 6 larvae (3 dpf).

(C) Confocal images of the cross-section of *Tg(krt18:mcherry;itgb4:tagBFP-nfsB)* at 24 hpf. The expression of *itgb4* is only detected in the basal layer. Scale bar, 20 μm.

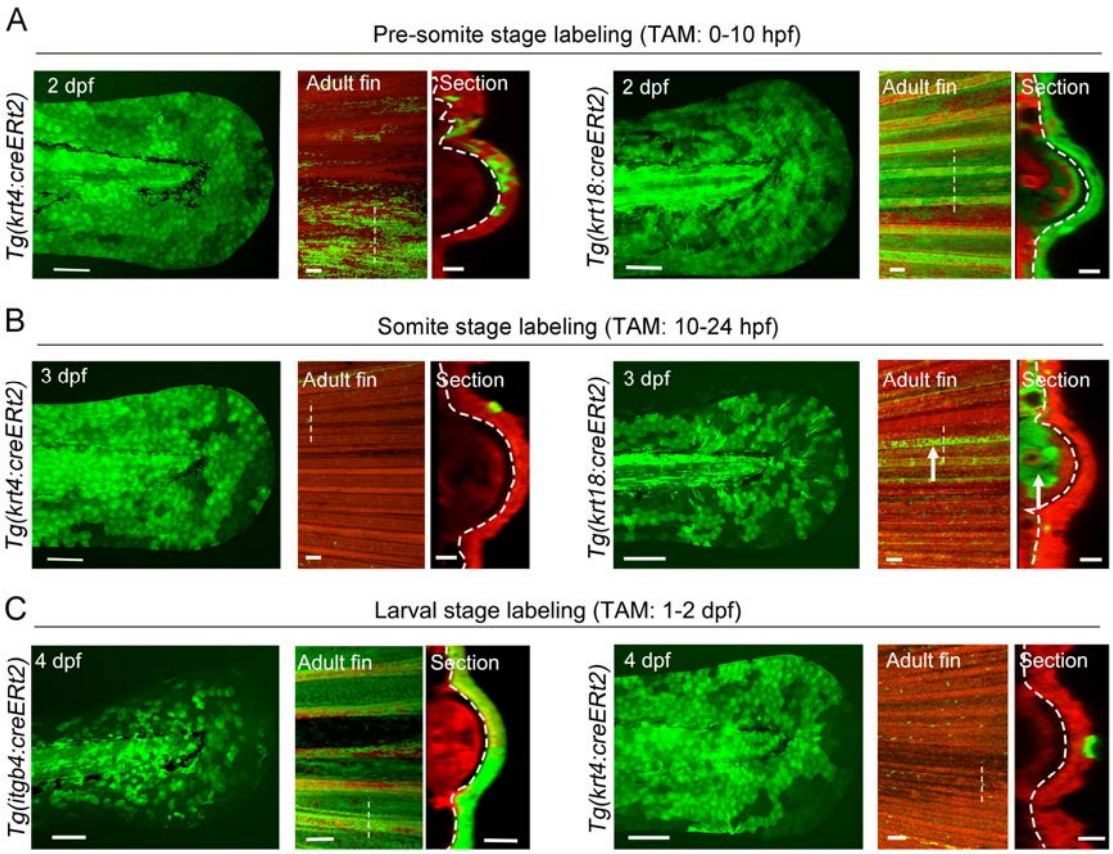


## Fig. 17. Fate segregation of basal cells from embryonic epithelial cells

(A) Tracking of epithelial cells that are *krt4*$^{+}$ or *krt18*$^{+}$ in the pre-somite stage. TAM (1 μM) treatment was done during 0-10 hpt. In both *Tgs*, progenies of EGFP-labeled cells were maintained in the adult fin epidermis including the basal cells and keratinocytes. (B) Tracking of epithelial cells that are *krt4*$^{+}$ or *krt18*$^{+}$ in the somite stage. EGFP$^{+}$ cells were induced at 3 dpf (left). In contrast to (A), progenies of labeled cells disappeared by the adult stage in both *Tgs* except a few remaining surface keratinocytes. In *krt18:cre*-labeling,

a group of mesenchymal cells that were maintained until the adult stage were observed (arrows).

(C) Tracking of epithelial cells that are *krt4*$^{+}$ or *itgb4*$^{+}$ during 1-2 dpf. The progenies of *itgb4*$^{+}$ cells contribute to the adult epidermis (left panels), whereas the progeny of *krt4*$^{+}$ cells mostly disappeared by the adult stage (right panels). Scale bars, 100 μm (2-4 dpf larva), 100 μm (adult fin), 50 μm (section).

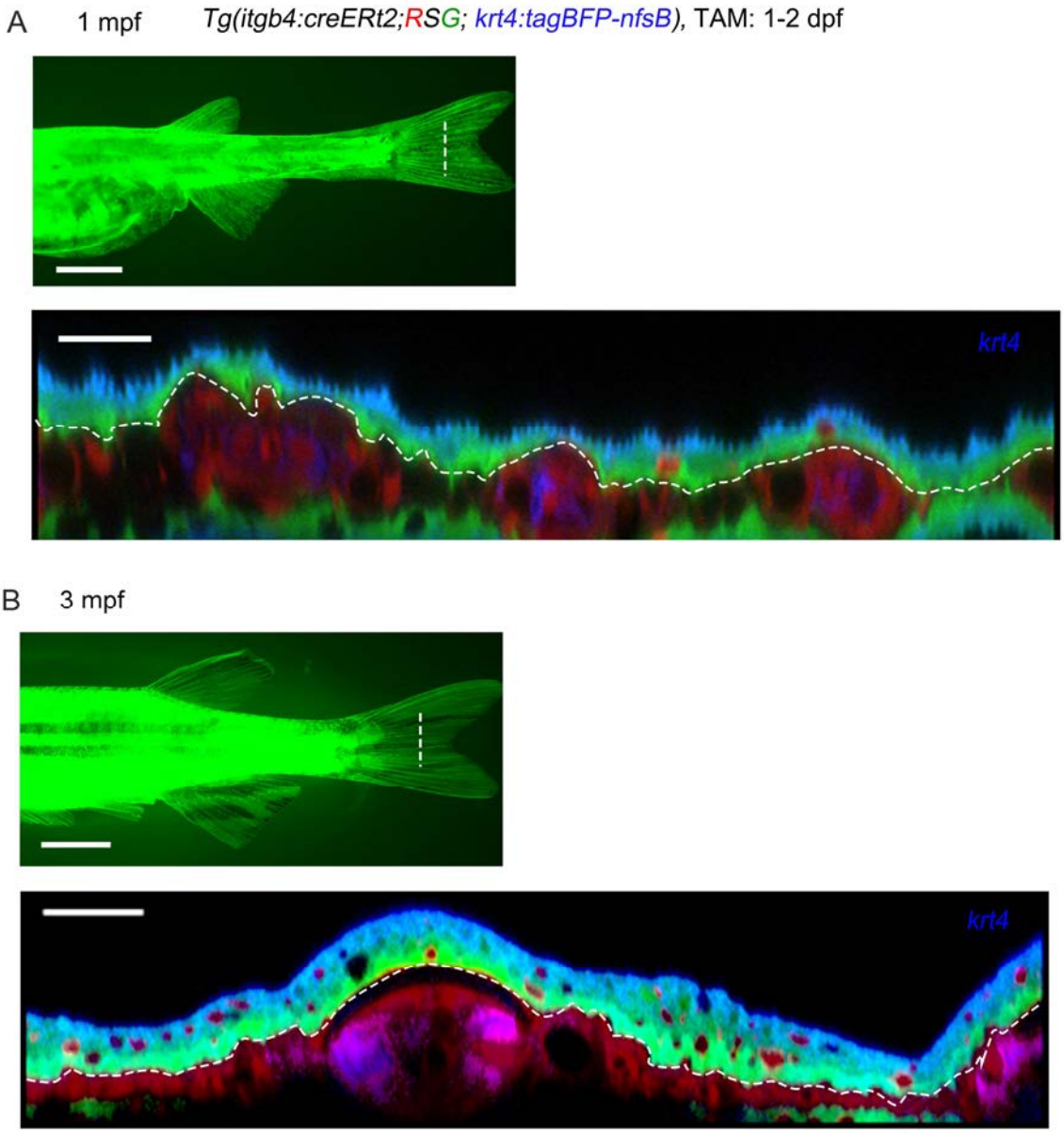


**Fig. 18. Progenies of embryonic *itgb4*$^{+}$ cells contribute to the adult epidermis throughout life**

Fluorescent images of *Tg(itgb4:creERt2;krt4:tagBFP-nfsB)* and confocal optical sections of the caudal fin. *itgb4*$^{+}$ cells were labeled at 1-2 dpf with 1μM TAM. The progenies of EGFP$^{+}$

labeled cells contributed to the entire epidermis in juvenile (1-month-old) and adult fish (3-month-old). Broken lines in the whole fish view, positions of optical section. Dotted lines in the optical section, basement membrane. Scale bars, 500 μm (A, upper panel), 1 mm (B, upper panel), 20 μm (sections).

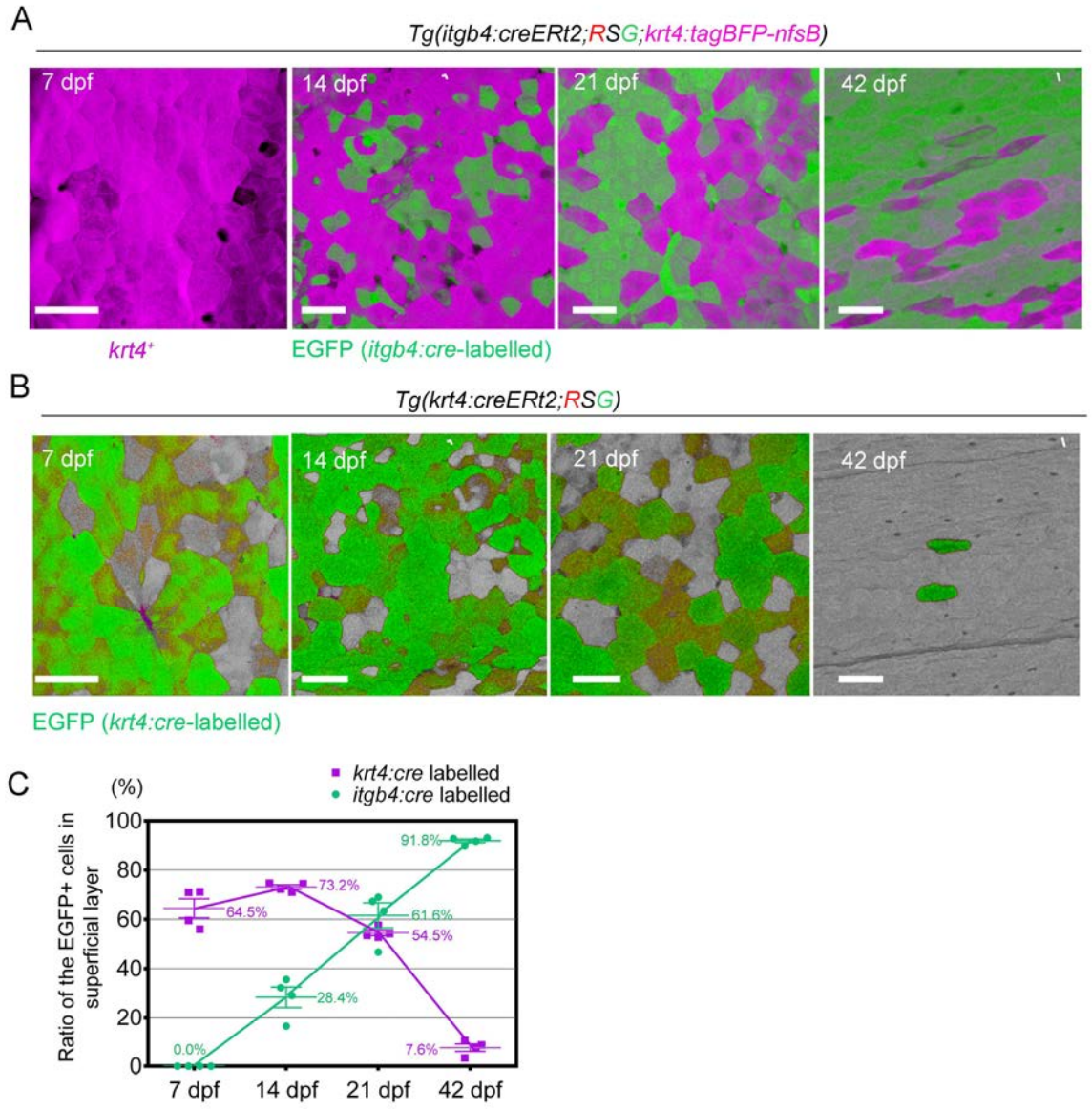


## Fig. 19. Tracking of the *itgb4*$^{+}$ and *krt4*$^{+}$ cells

(A) Confocal images of the progeny of *itgb4:cre*-labeled cells (TAM 1-2 dpf). The labeled basal cells proliferated to occupy over 90% of the epithelial cells until 42 dpf. Scale bars, 20 μm.

(B) Confocal images of the progeny of *krt4:cre*-labeled cells (TAM 1-2 dpf). In contrast to (A), their progenies nearly disappeared by 42 dpf. Scale bars, 20 μm

(C) Statistical analysis of (A, B). The embryonic *krt4*$^{+}$ epithelial cells were gradually replaced by the keratinocytes derived from *itgb4*$^{+}$ basal cells. n > 250 cells (A, B) in the superficial layer from 4 fish, respectively. Data are presented as mean ± s.e.m.

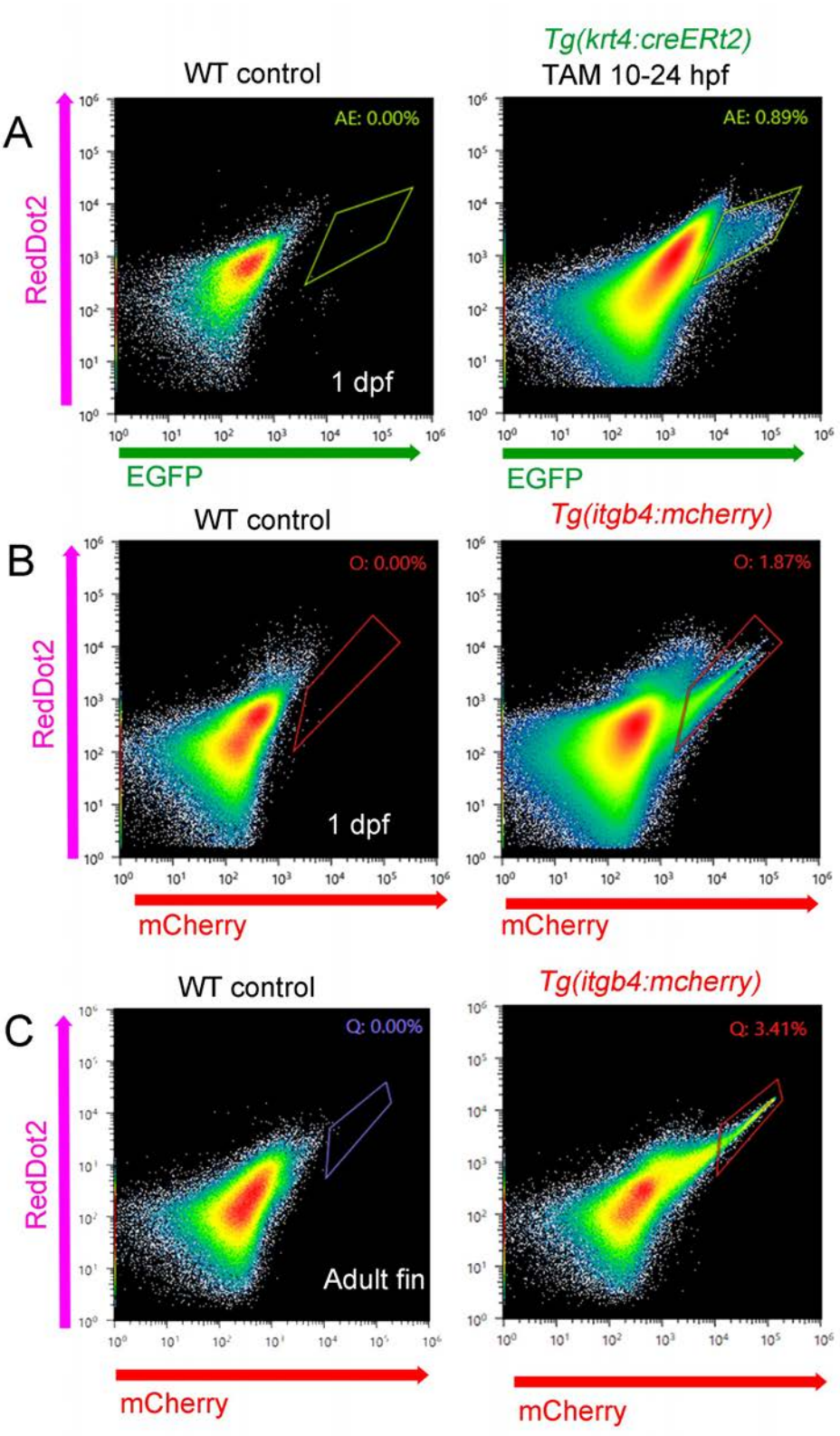
A
WT control
Tg(krt4:creERt2)
TAM 10-24 hpf
AE: 0.00%
AE: 0.89%
RedDot2
1 dpf
EGFP
EGFP
B
WT control
Tg(itgb4:mcherry)
O: 0.00%
O: 1.87%
RedDot2
1 dpf
mCherry
mCherry
C
WT control
Tg(itgb4:mcherry)
Q: 0.00%
Q: 3.41%
RedDot2
Adult fin
mCherry
mCherry

## Fig. 20. Fluorescent-activated cell sorting of embryonic *itgb4*$^{+}$, *krt4*$^{+}$ epithelial cells and adult *itgb4*$^{+}$ basal cells

(A) Fluorescent-activated cell sorting of *krt4*:*cre*-labeled epithelial cells (TAM, 10-24 hpf), which have the disappearing fate.

(B) Sorting of the *itgb4*$^{+}$ basal cell progenitors from 1 dpf embryos.

(C) Sorting of the *itgb4*$^{+}$ basal cells from the adult fin. RedDot2, dead cell marker. The dead cells are already excluded from the plots. Wild-type zebrafish embryos or adult fins were used for respective negative controls. Gating of EGFP$^{+}$ (polygon: AE) or mCherry$^{+}$ cells (polygon: O, Q) was determined based on the respective negative controls.

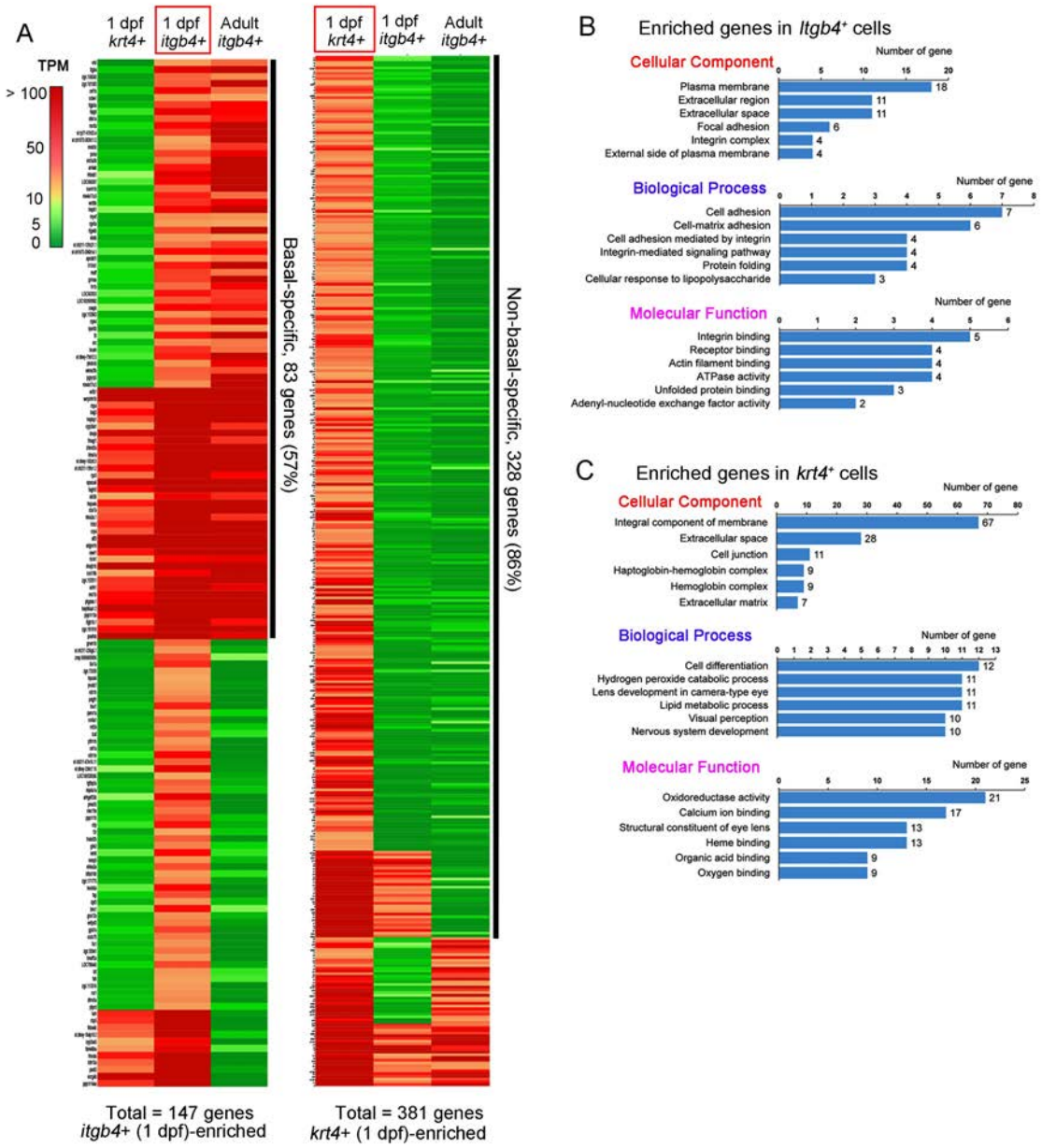


## Fig. 21. Basal cell identity is evident soon after the cell fate decision

(A) Heatmap of the average TPM values of enriched genes in embryonic *itgb4*$^{+}$ cells (147 genes, left panel) and *krt4*:*cre*-labeled cells (381 genes, right panel). These genes were

identified by a filter: TPM value (average of two independent experiments) > 10, fold change (1 dpf *krt4:cre*-labeled cells v.s. 1 dpf *itgb4*$^{+}$ cells) > 5. The red color in the heatmap represents the significantly high expression (TPM >10). Among the *itgb4*$^{+}$-enriched genes, 83 genes (57%) were also common in the adult *itgb4*$^{+}$ basal cells, suggesting that the basal cell character is already evident soon after the fate segregation at 1 dpf. Among the enriched genes in *krt4:cre*-labeled cells, 328 genes of them (86%) showed a low expression in the adult basal cells, indicating that these genes are specific to non-basal cells.

(B, C) Gene Ontology (GO) enrichment analysis of 83 basal genes (B) and 328 non-basal genes (C), respectively. The top 6 significantly enriched GO terms are represented in cellular components, biological processes, and molecular functions.

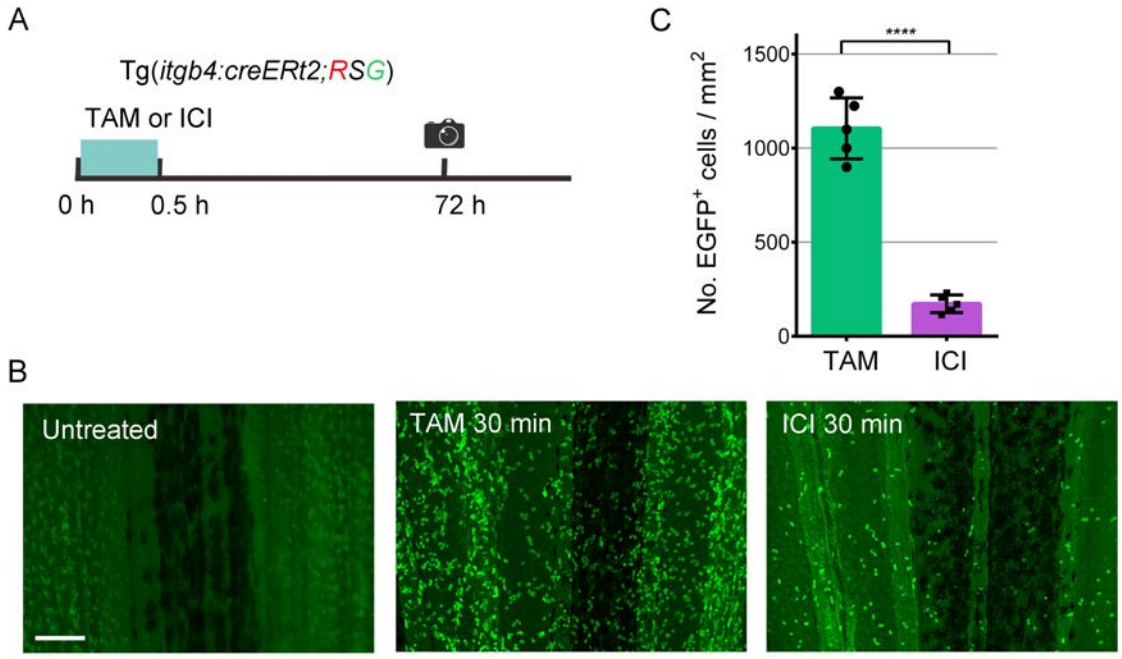


## Fig. 22. Sparse labeling of *itgb4*$^{+}$ basal cells by ICI

(A) Scheme of the experimental procedure. Adult fish was treated with 0.5 μM ICI or 0.5 μM TAM for 30 min.

(B) EGFP-expressing cells at 72 hpl after TAM or ICI treatment. In ICI treatment, only a small number of cells are labeled to allow single-cell tracking. Scale bar, 100 μm.

(C) Quantification of the EGFP+ cells in (B). n = 5 fish. Error bars denote mean ± s.e.m. Student's t-test (two-tailed) was performed to assess statistical significance. ****p < 0.0001.

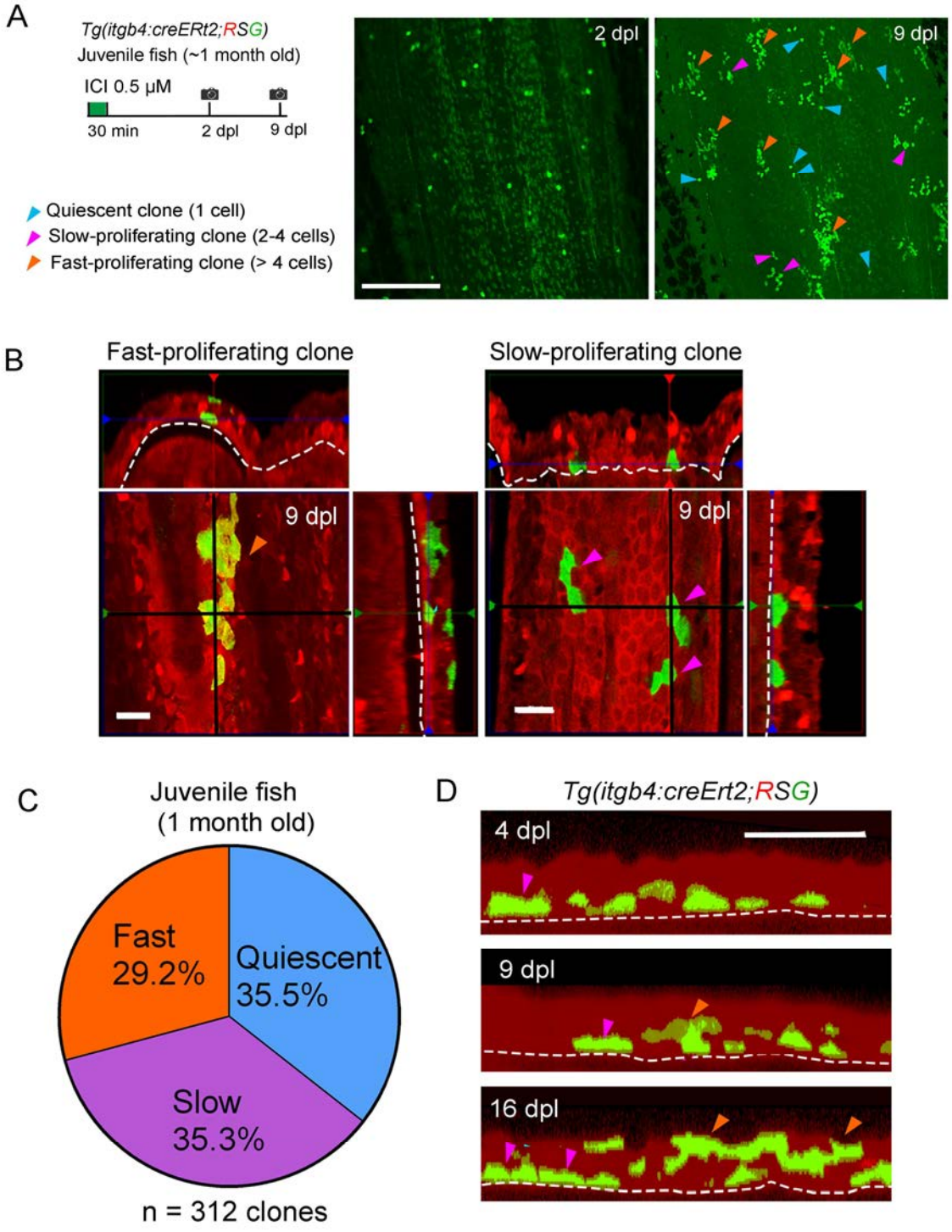
A
Tg(itgb4:creERt2;RSG)
Juvenile fish (~1 month old)
ICI 0.5 μM
30 min
2 dpl
9 dpl
Quiescent clone (1 cell)
Slow-proliferating clone (2-4 cells)
Fast-proliferating clone (> 4 cells)
2 dpl
9 dpl
B
Fast-proliferating clone
Slow-proliferating clone
9 dpl
9 dpl
C
Juvenile fish
(1 month old)
Fast
29.2%
Quiescent
35.5%
Slow
35.3%
n = 312 clones
D
Tg(itgb4:creErt2;RSG)
4 dpl
9 dpl
16 dpl

## Fig. 23. Different proliferative patterns of basal cells in the juvenile fish

(A) Tracking of the *itgb4:cre*-labeled cells at a single cell resolution in the 1-month-old juvenile fish. Fish were treated with 0.5 μM ICI to sparsely label the *itgb4*$^{+}$ basal cells. dpl, days post labeling. In a 1-week time window (2-9 dpl), the EGFP$^{+}$ cells displayed three proliferation patterns: quiescent (1 cell, blue arrowheads), slow-proliferating (2-4 cells, purple arrowheads), and fast-proliferating (> 4 cells, orange arrowheads). Note that the fast-proliferating clone contains both the basal cells and surface keratinocytes, while the slow-proliferating clone only contains the basal cells. Scale bar, 200 μm.
(B) Confocal images and their optical sections of fast-proliferating and slow-proliferating clones in the juvenile fish fin. Scale bars, 20 μm.
(C) Ratios of clones with respective proliferation patterns (n = 312 clones from 5 juvenile zebrafish).
(D) Confocal optical sections showing the distribution of *itgb4:cre*-labeled cells over time. Scale bar, 50 μm.

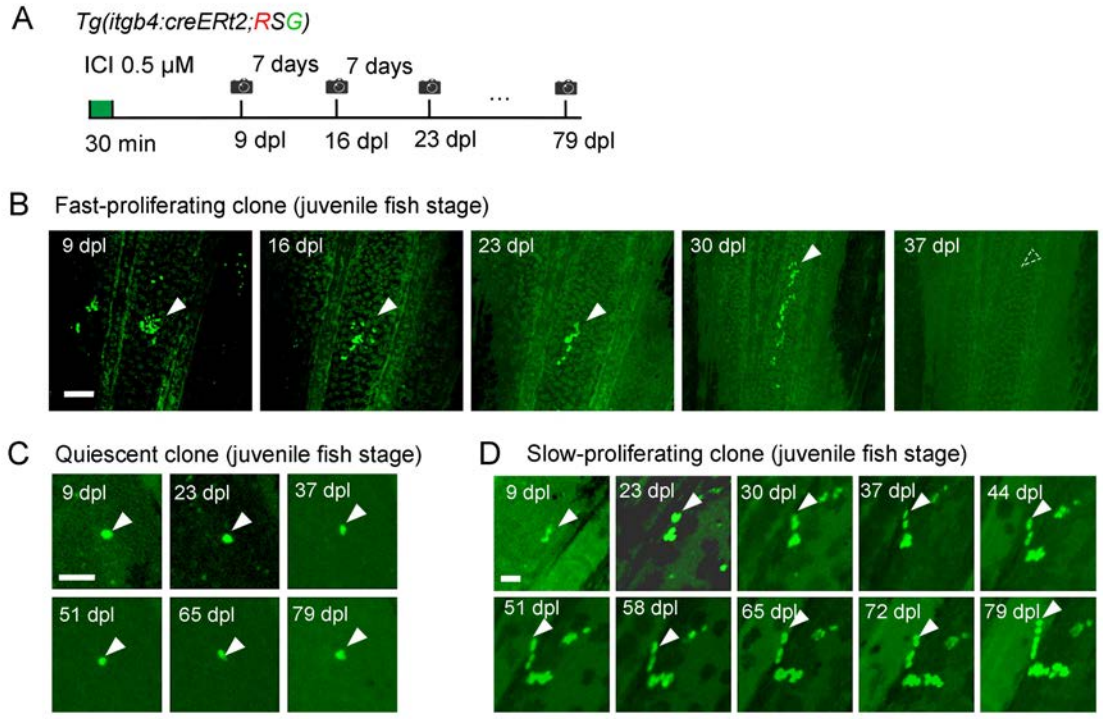


## Fig. 24. Long-term tracking of the basal cells with different proliferated patterns in juvenile fish

(A) Experimental scheme. Time-lapse images were taken at intervals of 7 days.

(B) Representative images of fast-proliferating clones, which quickly proliferated, but finally disappeared in the long run, suggested that such clones did not contain the basal stem cells. Scale bar, 100 μm.

(C) Representative image of quiescent clone. These clones kept quiescent more than 79 dpl. Scale bar, 50 μm.

(D) Representative image of slow-proliferating clone, which slowly expanded the clone size and maintained for more than 79 days. Scale bar, 30 μm.

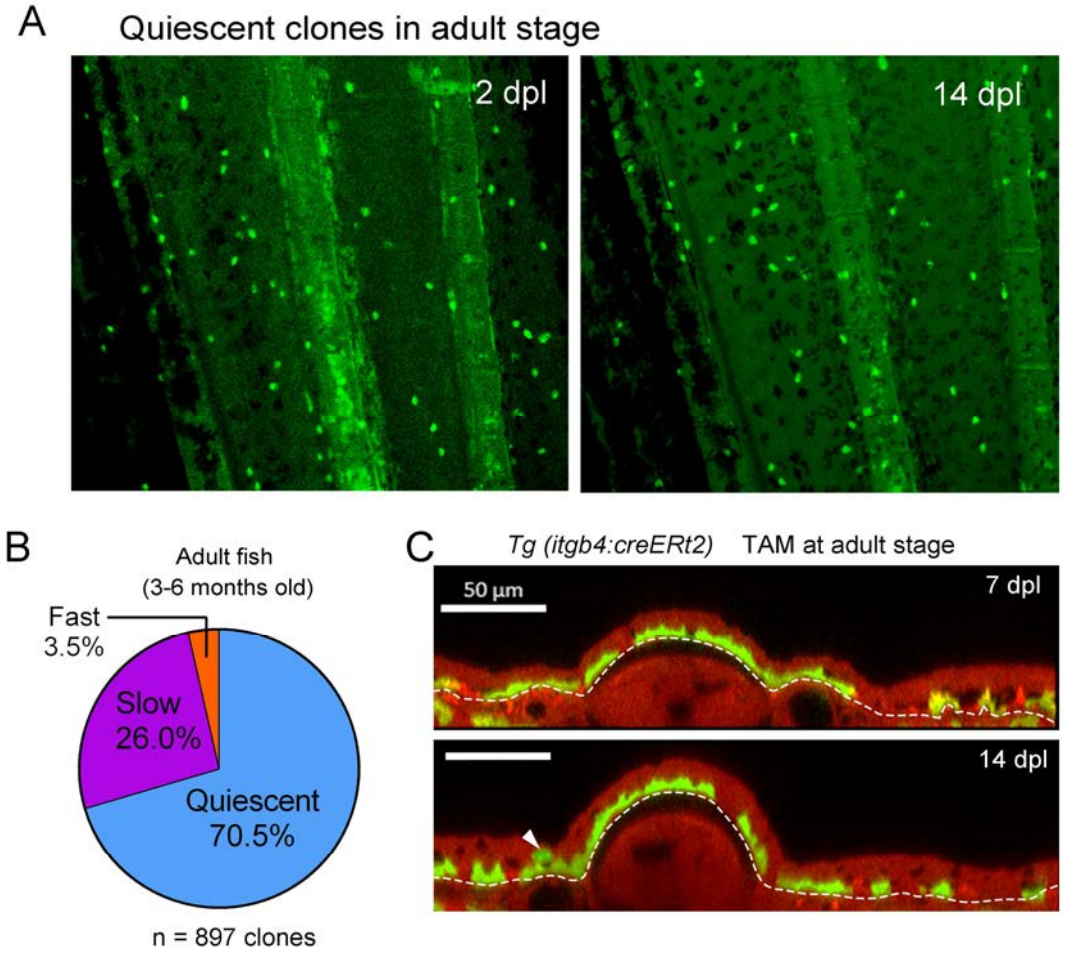


**Fig. 25. Basal cells mostly keep a quiescent state in the adult fish skin**

(A) Tracking of the *itgb4:cre*-labeled cells at a single cell resolution in adult fish (3 months old). Most of the labeled clones were quiescent in a time window between 2-16 dpl.

(B) Ratios of clones with respective proliferation patterns in the adult epidermis (n = 897 clones from 6 adult zebrafish).

(C) Confocal optical sections of *itgb4:cre*-labeled cells in the adult epidermis. Basal cells were labeled with TAM treatment. The basal cells did not produce the non-basal cells. Scale bar, 50 μm. Brocken lines, basement membrane.

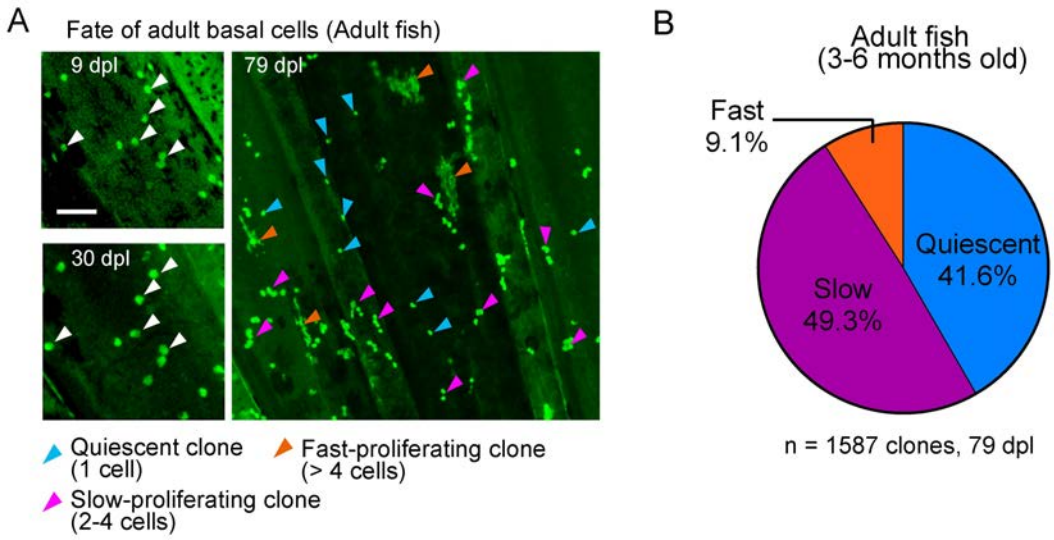


## Fig. 26. Long-term tracking of the basal cells in adult fish

(A) Tracking of the basal cells in a homeostatic condition of adult zebrafish. Images of 9 dpl and 30 dpl show the same region of the epidermis, where white arrowheads mark the corresponding cells. Colored arrowheads in 79 dpl point to the cells with different proliferation patterns, respectively. Scale bar, 50 μm.

(B) Ratios of basal cell behavior in (A) (n = 1587 clones from 3 adult fish). Most of the *itgb4*$^{+}$ basal cells were quiescent (41.6%) or slow-proliferating fate (49.3%). Only a small number of cells took the fast-proliferating fate (9.1%) by 79 dpl.

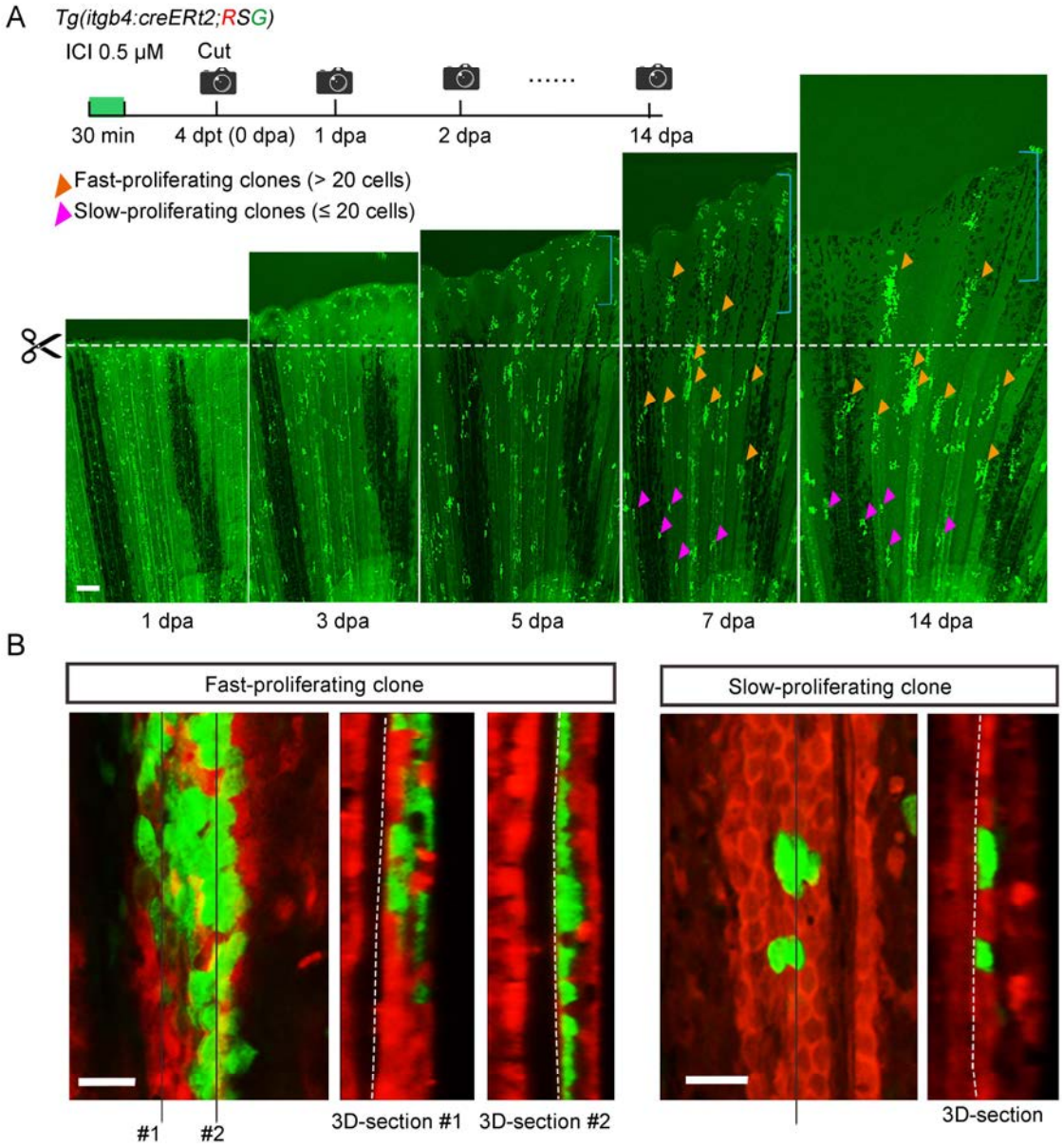


## Fig. 27. Basal cells are activated during fin regeneration

(A) Tracking of the basal cells until 14 days post-amputation (dpa). The *itgb4*$^{+}$ basal cells were sparsely labeled by ICI before amputation. As shown by Shibata et al. (2018) using the *Tg(fn1b:creERt2)*, the clones close to the amputation site (brackets) mostly disappeared by 2

weeks post-amputation. Broken line, amputation site. Among the clones that remain in the tissue for more than 2 weeks, the fast-proliferating cells (orange arrowheads) are located in the distal region, while the slow-proliferating ones (purple arrowheads) are in the proximal region. Scale bar, 300 μm.

(B) Confocal images and their optical sections of fast- and slow-proliferating clones. Slow proliferating clones contain only the basal cells as in the juvenile fish and homeostatic condition. Interestingly, the fast-proliferating clones in regenerating fin contained both differentiated keratinocytes and basal cells, suggesting that self-renew and differentiation of basal cells almost simultaneously take place. Black lines indicate the planes of optical sections. Broken lines, basement membrane. Scale bars, 20 μm.

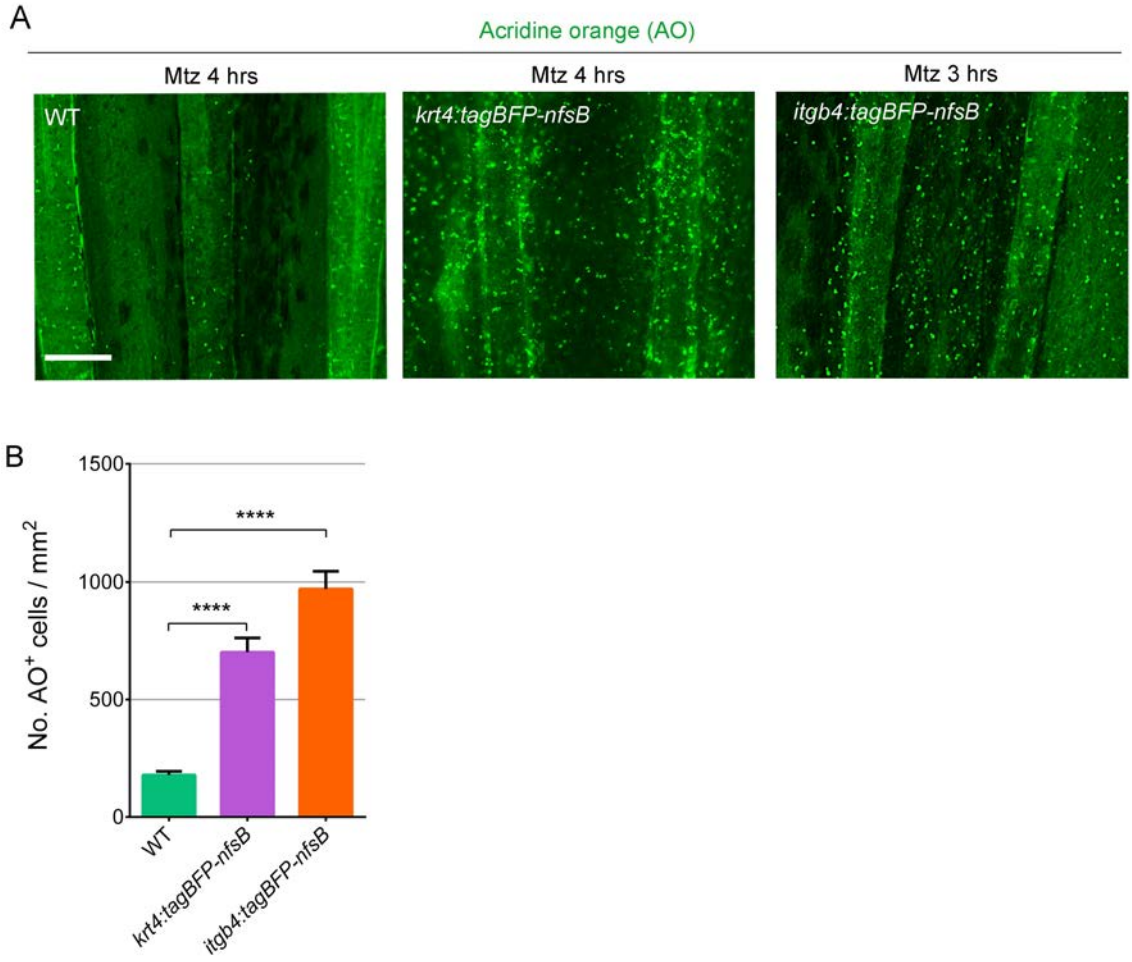


**Fig. 28. Detection of cell death after Mtz treatment.**

(A) Detection of cell death by acridine orange (AO) staining of adult fin after Mtz treatment. Dead cells increased after 4 hrs of Mtz treatment in *Tg(krt4:tagBFP-nfsB)* and 3 hrs of Mtz treatment in *Tg(itgb4:tagBFP-nfsB)*. Scale bar, 100 μm.

(B) Quantification of $AO^+$ cells in (A). Numbers were counted from areas of the same size. n = 5 regions (0.5 $mm^2$) of the fin from 5 fish respectively. Error bars denote the mean and s.e.m. Student's t-test (two-tailed) was performed to assess statistical significance. $^{****}p <$ 0.0001.

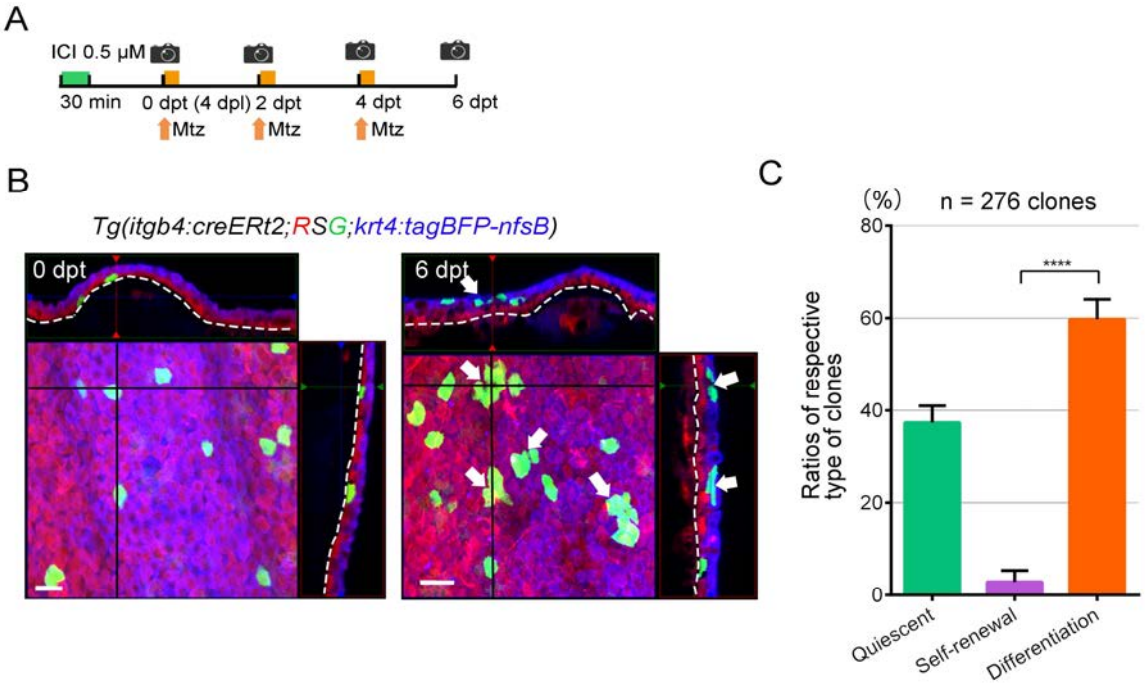


## Fig. 29. Induction of basal cell differentiation by non-basal keratinocyte injury

(A) Experimental procedure of basal cell labeling and *krt4*$^{+}$ cell injury. Mtz, metronidazole treatment.

(B) Confocal images and their optical sections of the EGFP-labeled basal cells in the adult fin before (left panel) and after non-basal cell injury (6 dpt, right panel). Brocken lines, basement membrane. dpt, day post treatment. After injury of *krt4*$^{+}$ cells, the basal cells often became the *krt4*$^{+}$ keratinocytes at 6 dpt. Note that such clones did not contain the basal cells, indicating that the basal cells differentiated into non-basal cells.

(C) Quantification of the basal cell reactions in response to non-basal cell injury. The number of clones was counted on confocal images (n = 276 clones from 4 adult fins). Error bars denote mean ± s.e.m. Student's t-test (two-tailed) was performed to assess statistical significance. $^{****}p < 0.0001$.

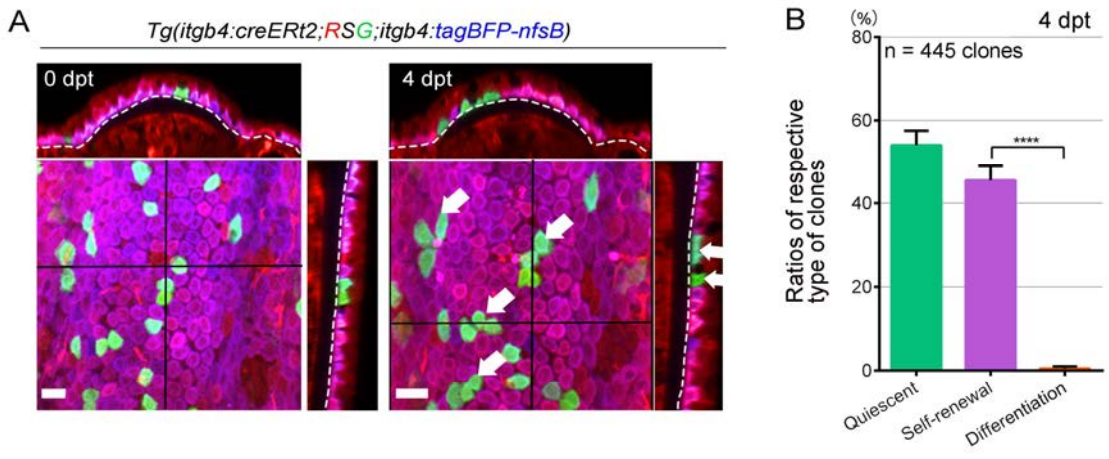


## Fig. 30. Induction of basal cell self-renewal by basal cell injury

(A) Confocal images and their optical sections of the EGFP-labeled basal cells in the adult fin before (left panel) and after basal cell injury (4 dpt, right panel). Broken lines, basement membrane. After the injury of *itgb4*$^{+}$ basal cells, many of the labeled-basal cells stayed in the basal layer. They either remained quiescent or slowly proliferated to self-renew the basal cells (arrows).

(B) Quantification of the basal cell reactions in response to basal cell injury. The number of clones was counted on confocal images (n = 445 clones from 4 adult fins). Error bars denote mean ± s.e.m. Student's t-test (two-tailed) was performed to assess statistical significance. $^{****}p < 0.0001$.

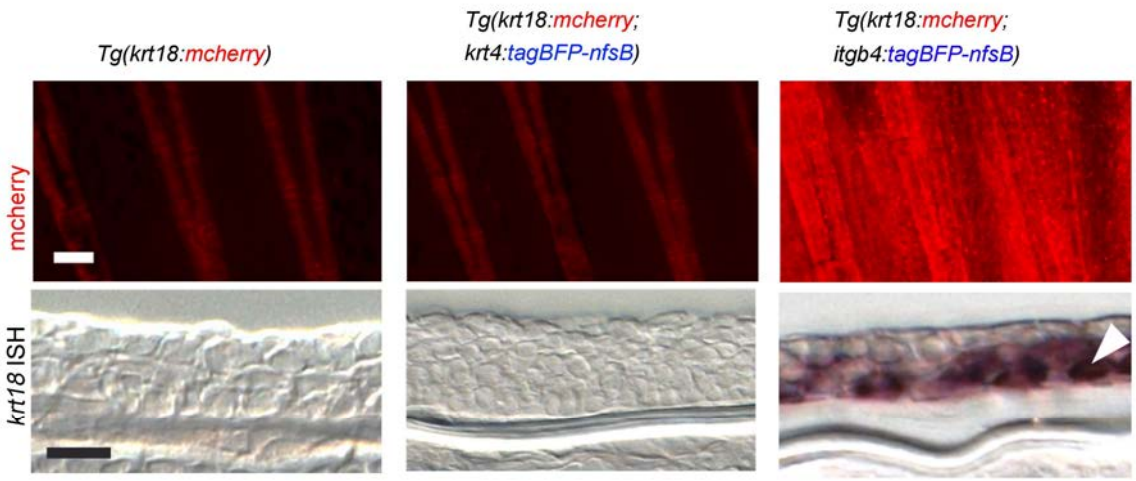


## Fig. 31. The *krt18* expression is induced under *itgb4*$^{+}$ basal cell ablation

Induction of *krt18* expression after basal cell injury but not by the keratinocyte injury as revealed by *Tg(krt18:mcherry)* (upper panels) and ISH analyses (longitudinal fin sections, lower panels). All images were at 1 dpt. *krt18* expression was only induced by the basal cell injury. Scale bar, 100 µm (upper panels), 20 µm (lower panels). Arrowhead, *krt18*$^{+}$ cells in the basal layer.

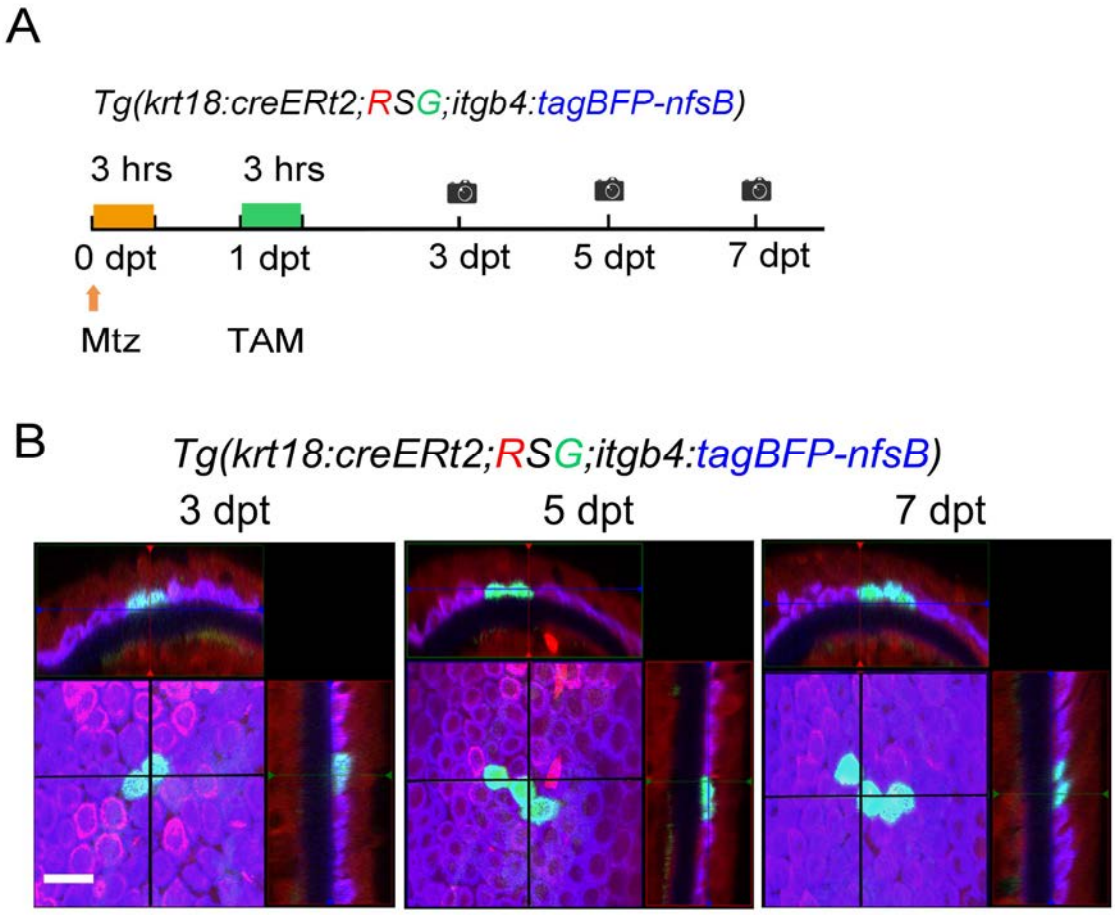


**Fig. 32. The *krt18*-expressed basal cells undergo self-renewal after *itgb4*$^{+}$ basal cell ablation**

(A) Experimental procedure of basal cell injury and the following *krt18*$^{+}$ cell labeling.

(B) Tracking of *krt18*-expressed cells that were induced by basal cell injury. Most of the labeled cells underwent self-renewal to replenish the *itgb4*$^{+}$ basal cells (n = 66 out of 75 clones from 5 fish). The assessment was done by the number of cells at 7 dpt and confocal 3D imaging. Scale bar, 20 μm.

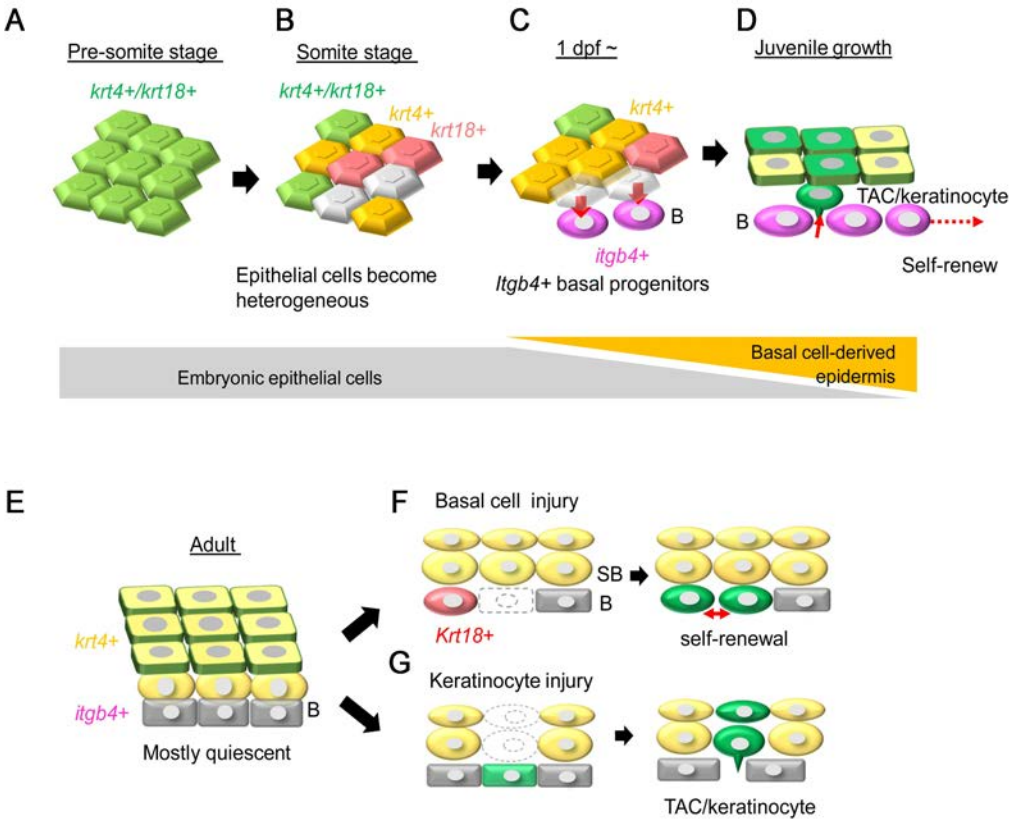


## Fig. 33. Schematic summary of the life cycle of epidermal basal stem cells

(A) The *krt4* and *krt18* are expressed uniformly in epithelial cells before the somite stage.

(B) At the somite stage, the epidermal cells become heterogeneous with different combinations of *krt18* and *krt4* expression.

(C) A fraction of epithelial cells with decreased expression of *krt18* and *krt4* become *itgb4*$^{+}$.

(D) In the subsequent stage, the *itgb4*$^{+}$ cells frequently produce new basal cells and TACs/keratinocytes to replace the embryonic epithelial cells.

(E) At the adult stage, many of the *itgb4*$^{+}$ basal cells become in a quiescent state.

(F) Basal cell injury only induces the basal cell self-renewal by way of the *krt18*$^{+}$ state.

(G) The *krt4*$^{+}$ non-basal cell injury activates the basal cell differentiation to produce the TACs/keratinocytes**.**